PLEASE CITE THIS ARTICLE AS DOI: 10.1063/5.0160331

## Classes of O-D centers in unintentionally and Fe-doped β-Ga<sub>2</sub>O<sub>3</sub> annealed in a D<sub>2</sub> ambient

Amanda Portoff,<sup>1</sup> Andrew Venzie,<sup>1</sup> Michael Stavola,<sup>1,a)</sup> W. Beall Fowler,<sup>1</sup> Evan Glaser,<sup>2</sup> and Stephen J. Pearton<sup>3</sup>

<sup>1</sup>Department of Physics, Lehigh University, Bethlehem, Pennsylvania 18015, USA <sup>2</sup>U.S. Naval Research Laboratory, Electronics Science and Technology Division Code 6880, Washington, DC 20375

<sup>3</sup>Department of Materials Science and Engineering, University of Florida, Gainesville, Florida 32611, USA

## **ABSTRACT**

β-Ga $_2$ O $_3$  has attracted much recent attention as a promising ultrawide bandgap semiconductor. Hydrogen can affect the conductivity of β-Ga $_2$ O $_3$  through the introduction of shallow donors and the passivation of deep acceptors. The introduction of H or D into β-Ga $_2$ O $_3$  by annealing in an H $_2$  or D $_2$  ambient at elevated temperature produces different classes of O-H or O-D centers. This work is a study of the interaction of D with  $V_{Ga1}$  and  $V_{Ga2}$  deep acceptors as well as other impurities and native defects in Ga $_2$ O $_3$  by infrared spectroscopy and complementary theory. (We focus primarily on the deuterium isotope of hydrogen because the vibrational modes of O-D centers can be detected with higher signal-to-noise ratio than those of O-H.) O-D centers in β-Ga $_2$ O $_3$  evolve upon annealing in an inert ambient and are transformed from one type of O-D center into another. These reactions affect the compensation of unintentional shallow donors by deep acceptors that are passivated by D. Defects involving additional impurities in β-Ga $_2$ O $_3$  compete with  $V_{Ga}$  deep acceptors for D and modify the deuterium-related reactions that occur. The defect reactions that occur when D is introduced by annealing in a D $_2$  ambient appear to be simpler than those observed for other introduction methods and provide a foundation for understanding the D-related reactions that can occur in more complicated situations.

Corresponding author: a)michael.stavola@Lehigh.edu

PLEASE CITE THIS ARTICLE AS DOI: 10.1063/5.0160331

## I. INTRODUCTION

 $\beta$ -Ga<sub>2</sub>O<sub>3</sub> has a band-gap energy of 4.9 eV and shows great promise for next-generation, high-power and deep-UV devices.<sup>1-5</sup> Defects and impurities in  $\beta$ -Ga<sub>2</sub>O<sub>3</sub> that determine its electrical properties are being investigated extensively.<sup>6</sup> Hydrogen impurities in semiconducting oxides and their interactions with other defects strongly affect conductivity.<sup>7-9</sup> This is also the case for H in  $\beta$ -Ga<sub>2</sub>O<sub>3</sub><sup>6,10,11</sup> where H centers have their own unique behaviors that continue to be revealed.

The implantation of H into  $\beta$ -Ga<sub>2</sub>O<sub>3</sub> introduces both H and native defects with which it interacts. Similarly, the introduction of H by H-plasma exposure introduces both H and native defects. In another recent study, the defects that H can interact with have been manipulated by pre-annealing samples under oxygen or Ga-rich conditions prior to the introduction of H to produce surprising effects on the electrical properties of  $\beta$ -Ga<sub>2</sub>O<sub>3</sub>. In

Furthermore, the introduction of H into unintentionally doped  $\beta$ -Ga<sub>2</sub>O<sub>3</sub> by annealing in an H<sub>2</sub> ambient at elevated temperature has been found to introduce several O-H centers.<sup>19-21</sup> However, the interaction with native defects appears to be simpler in this case and to be dominated by reactions of H with  $V_{Ga}$  centers. [ $\beta$ -Ga<sub>2</sub>O<sub>3</sub> has two inequivalent Ga sites, Ga(1) that is tetrahedrally coordinated and Ga(2) that is octahedrally coordinated.<sup>1,2,4</sup>]

The  $V_{Ga}$  centers in turn exhibit several "split" structures, the first noted by Varley *et al.*<sup>22</sup> and others by Kyrtsos *et al.*<sup>23</sup> who denoted them as "a", "b", and "c." In these cases, one neighboring Ga moves into an interstitial site adjacent to the original vacancy, resulting in a vacancy – interstitial – vacancy configuration which may be lower in energy than the unshifted vacancy.<sup>24</sup>

IR absorption spectroscopy measured with polarized light for H in  $Ga_2O_3$  has revealed a dominant O-H center that gives rise to a vibrational line at 3437 cm<sup>-1</sup> with distinctive properties in samples that contain both H and D.<sup>19,20</sup> Theory has assigned the 3437 cm<sup>-1</sup> line to a  $V_{Ga1}^{ib} - 2H$  complex with two H atoms trapped by a split Ga(1) vacancy with the "b" configuration,  $V_{Ga1}^{ib}$ . Similarly, D in  $Ga_2O_3$  gives rise to a D line at 2546 cm<sup>-1</sup> that was assigned to a  $V_{Ga1}^{ib} - 2D$  complex.<sup>19</sup> The split structures have also been observed by electron paramagnetic resonance<sup>25,26</sup> and scanning transmission electron microscopy.<sup>27</sup> Positron annihilation results for  $\beta$ - $Ga_2O_3$  have also been found to be dominated by split  $Ga_1$ 0 vacancies.<sup>28</sup>

Additional O-H (O-D) lines that are less thermally stable have also been discovered.<sup>20</sup> These O-H (O-D) centers were not seen in early experiments<sup>19</sup> performed for wafers with a

PLEASE CITE THIS ARTICLE AS DOI: 10.1063/5.0160331

 $(\bar{2}01)$  face because several have transition moments perpendicular to  $(\bar{2}01)$ . To explain their polarization properties, several of these lines have been assigned to H (D) trapped at a relaxed  $V_{Ga1}$  center with the split "c" configuration<sup>21</sup>,  $V_{Ga1}^{ic}$ .

 $\beta$ -Ga<sub>2</sub>O<sub>3</sub> hydrogenated by annealing in an H<sub>2</sub> ambient has also been studied recently by deep level transient spectroscopy (DLTS) and a broad DLTS peak labeled E1 was produced.<sup>21</sup> The assignment of E1 to overlapping DLTS peaks arising from H-containing complexes with similar structures was suggested.

In the present paper, the combination of vibrational spectroscopy<sup>29,30</sup> and free-carrier absorption<sup>31,32</sup> is used to further investigate the O-H and O-D centers that are formed in  $\beta$ - Ga<sub>2</sub>O<sub>3</sub> by annealing in an H<sub>2</sub> or D<sub>2</sub> ambient, their reactions upon annealing, and their effect on conductivity. These results provide a foundation for understanding more complex situations where additional defects from implantation, plasma exposure, and annealing pretreatments also are involved.

β-Ga $_2$ O $_3$  can be doped with Fe to produce semi-insulating substrates. Impurities in β-Ga $_2$ O $_3$  can act as traps for H that compete with  $V_{Ga}$  defects. We have introduced H and D into a heavily Fe-doped β-Ga $_2$ O $_3$  sample grown by the Czochralski method to investigate the trapping of H or D by impurities and the defect reactions that occur upon annealing. The behaviors of H and D in undoped and intentionally Fe-doped β-Ga $_2$ O $_3$  samples are compared and contrasted.

In most studies, no O-H (O-D) absorption had been reported for O-H (O-D) centers with a component of their transition moment along the "b" axis, i.e. with **E**//[010], 19,20,34-36,38 so there has been a focus on O-H (O-D) centers with H (D) trapped at different configurations of a split Ga(1) vacancy. However, O-D lines at 2475 and 2493 cm<sup>-1</sup> with a component of their polarization along the [010] direction have been discovered recently, leading to their assignment to O-D trapped at a Ga(2) vacancy.<sup>39</sup> Additional results for O-D centers of this type are also presented here.

## II. EXPERIMENTAL METHODS

Unintentionally-doped  $\beta$ -Ga<sub>2</sub>O<sub>3</sub> wafers (n-type with N<sub>D</sub>-N<sub>A</sub> nominally <9x10<sup>17</sup> cm<sup>-3</sup>) with both (010) and ( $\bar{2}01$ ) faces were purchased from the Tamura Corporation. Additional  $\beta$ -Ga<sub>2</sub>O<sub>3</sub> samples doped with Fe for our studies were grown by the Czochralski method at Synoptics.

## This is the author's peer reviewed, accepted manuscript. However, the online version of record will be different from this version once it has been copyedited and typeset PLEASE CITE THIS ARTICLE AS DOI: 10.1063/5.0160331

This (010) Fe-doped boule was 1 cm thick allowing thick samples with different orientations to be prepared. Bulk samples were hydrogenated by annealing at 900 °C for several hours in sealed quartz ampoules that contained  $H_2$  or  $D_2$  gas (~2/3 atm at room temperature). Ampoules were cooled in sand at room temperature following these treatments.  $H_2$  or  $D_2$  are presumed to dissociate at the sample surface and to diffuse in the sample as atomic species.<sup>11</sup>

Several samples were annealed in an inert ambient subsequent to their treatment in  $H_2$  or  $D_2$ . These anneals were performed in a tube furnace in a flowing Ar ambient and were terminated by placing the  $Ga_2O_3$  sample on an Al plate at room temperature.

Infrared (IR) absorption spectra were measured with a Nicolet iS50 Fourier transform IR spectrometer equipped with a  $CaF_2$  beamsplitter and a liquid  $N_2$ -cooled InSb detector. Samples were cooled for our measurements with liquid  $N_2$  in a Helitran continuous flow cryostat. The spectra for the D-centers have higher signal to noise ratio than the corresponding H spectra and so are featured in most of the data presented in this paper. Also note that when we refer generically to "hydrogen" in this paper rather than explicitly writing H or D, we are considering both hydrogen isotopes,  $^1H$  and  $^2H$ .

The polarization of the transmitted light was analyzed with a wire-grid polarizer placed after the sample. The in-plane orientations of our  $\beta$ -Ga<sub>2</sub>O<sub>3</sub> samples could be determined from the orientations of their (100) and (001) cleavage planes.

 $\beta$ -Ga $_2$ O $_3$  has a low-symmetry monoclinic structure  $^{40,41}$  that makes the vibrational absorption anisotropic. Polarized absorption measurements have been made for  $\beta$ -Ga $_2$ O $_3$  samples with either ( $\bar{2}01$ ), (010) or (100) faces to obtain information about the orientations of the transition moments of the different O-D centers that are of interest.  $\beta$ -Ga $_2$ O $_3$  is biaxial and has principal dielectric axes X, Y, Z. The Y axis is taken to be along the [010] optic axis. The frequency dependent orientations of the perpendicular X and Z axes were determined previously by ellipsometry over a broad spectral range. Polarized vibrational absorption measurements have also been used to determine the orientations of the X and Z axes in the IR range of interest here.  $^{36,43}$ 

## III. EXPERIMENTAL RESULTS

A. Vibrational spectra and their thermal stability for unintentionally doped β-Ga<sub>2</sub>O<sub>3</sub>

PLEASE CITE THIS ARTICLE AS DOI: 10.1063/5.0160331

Spectra are shown in Fig. 1 for an unintentionally doped  $\beta$ -Ga<sub>2</sub>O<sub>3</sub> sample with a ( $\overline{2}01$ ) face purchased from the Tamura Corp. that had been annealed in a D<sub>2</sub> ambient at 900°C for 6 h. A selection of spectra is presented that were measured following sequential annealing treatments (30 min) in an inert ambient at the temperatures indicated.

To be able to investigate the properties of all of the O-D centers, including those with a transition moment perpendicular to the  $(\bar{2}01)$  plane, the sample was rotated by 45° with respect to the direction of the incident light as is shown in the inset to Fig. 1. In this case, light polarized with  $\mathbf{E} \perp [102]$  for the rotated sample has an electric vector with a component normal to  $(\bar{2}01)$ . The upper spectra (shown in blue) were measured for the polarization with  $\mathbf{E}//[102]$ , i.e., with no component of the electric field perpendicular to the  $(\bar{2}01)$  face. The lower spectra (shown in black) were measured for the polarization with  $\mathbf{E} \perp [102]$ , and several additional O-D lines are revealed. The frequencies of the various O-D lines we have observed for this unintentionally doped sample are listed in Table 1 (in regular type face). The lines shown in Fig. 1 were seen previously by Qin *et al.* for a more complicated sample geometry that impeded a detailed annealing study.<sup>20</sup>

The selection of spectra in Fig. 1 and their annealing dependence in Fig. 2 show that all but the dominant line at 2546 cm<sup>-1</sup> is annealed away at a temperature of approximately 450°C. When these defects are annealed away, the 2546 cm<sup>-1</sup> line is greatly increased in strength, making the  $V_{Ga1}^{ib}-2D$  complex the primary sink for D in the sample. In these experiments in which D was introduced in the  $\beta$ -Ga<sub>2</sub>O<sub>3</sub> sample by annealing in a D<sub>2</sub> ambient, the 2546 cm<sup>-1</sup> line remains thermally stable up to an annealing temperature of 1000°C in an inert ambient.

In previous experiments in which H or D was introduced by ion implantation, the 2546 cm<sup>-1</sup> line disappeared for an annealing temperature of 450°C, suggesting its interaction with other defects introduced by the implantation.<sup>14,38</sup>

## B. Vibrational spectra and their thermal stability for Fe-doped β-Ga<sub>2</sub>O<sub>3</sub>

In another set of experiments, H or D were introduced into an intentionally Fe-doped sample grown by the Czochralski method<sup>37</sup> to investigate how an impurity with high concentration can affect the defect reactions that involve hydrogen. This sample was characterized by secondary ion mass spectrometry (SIMS) to determine the concentrations of a few common impurities in  $\beta$ -Ga<sub>2</sub>O<sub>3</sub>.<sup>44</sup> The SIMS profiles in Fig. 3 show that Fe is the dominant impurity in this deliberately doped sample with a concentration [Fe] =  $4 \times 10^{18}$  cm<sup>-3</sup>. Ir impurities introduced by the crucible

PLEASE CITE THIS ARTICLE AS DOI: 10.1063/5.0160331

## used for Czochralski growth also have a high concentration, [Ir] = $2x10^{18}$ cm<sup>-3</sup>. The concentration of Si is typical of $\beta$ -Ga<sub>2</sub>O<sub>3</sub> materials not intentionally doped with Si and is [Si] = $10^{17}$ cm<sup>-3</sup>.<sup>45</sup> Only a trace concentration of Mg is present. IR absorption spectra with polarizations $\mathbf{E}$ /[100] and $\mathbf{E}$ 100] are shown in Figs. 4(a) and

IR absorption spectra with polarizations E/[100] and  $E\perp[100]$  are shown in Figs. 4(a) and 4(b), respectively, for the (010) Fe-doped  $\beta$ -Ga<sub>2</sub>O<sub>3</sub> sample following deuteration by a high-temperature annealing treatment in a D<sub>2</sub> ambient. The [100] direction has been found to be close to the Z dielectric axis, and the direction perpendicular to [100] is close to the X dielectric axis. Subsequent to our absorption measurements, a piece of this sample was thinned by lapping and polishing until the O-D lines disappeared to show that the absorbing layers at the front and back (010) surfaces were 1.75 mm thick. These relatively thick deuterated layers allowed weak O-D lines to be detected.

A selection of the spectra is shown in Fig. 4 that were measured for a series of sequential anneals made in  $50^{\circ}$ C increments to probe the evolution of O-D centers in an Fe-doped  $\beta$ -Ga<sub>2</sub>O<sub>3</sub> sample. The dependence of the IR line intensities on the annealing temperature is shown in Fig. 5. The lines seen in Fig. 1 are also seen for the Fe-doped, Czochralski-grown sample along with several additional lines that were not seen in Fig. 1. These additional lines are also listed in Table I (bold italic typeface). A few lines were seen only for an annealing temperature near  $350^{\circ}$ C and are shown in Fig. 6 (with frequencies underlined and shown in blue).

The 2577 cm<sup>-1</sup> line was previously assigned to an OD-Si complex that was seen for a Sidoped epitaxial layer grown on an Fe-doped substrate that had been deuterated by D-plasma exposure. So both Fe and Si impurities were present in these samples. Our present results for a heavily Fe-doped sample show a strong dominant line at 2577 cm<sup>-1</sup> that suggests its possible assignment to an OD-Fe complex. However, there is also a substantial concentration of Si present in these samples as well. Definitive assignments of the 2577 and 2583 cm<sup>-1</sup> lines to complexes containing Fe or Si impurities are not yet possible.

The assignments of the numerous additional O-D lines remain even more uncertain. The 2631 cm<sup>-1</sup> line is strong in both the unintentionally-doped and Fe-doped  $\beta$ -Ga<sub>2</sub>O<sub>3</sub> samples. The Fe-doped sample grown by the Czochralski method shows several lines that were not seen in samples obtained from the Tamura Corp. suggesting that they could be impurity related. Our Czochralski-grown sample also contains a high concentration of Ir. Ritter *et al.* suggested that the O-D lines at 2463, 2556, and 2590 cm<sup>-1</sup> (10K) seen in their experiments could be due to OD-

PLEASE CITE THIS ARTICLE AS DOI: 10.1063/5.0160331

Ir complexes.<sup>34</sup> The spectra shown in Fig. 6 show lines at 2462 and 2555 cm<sup>-1</sup> (77K) which, following Ritter *et al.*, might indeed be due to OD-Ir complexes.

## C. Polarization dependence of the O-D lines

(i) Polarization in the (010) plane: Information about the orientations of the transition moments for the O-D centers that have been observed can be obtained from the polarization dependence of their O-D vibrational lines, providing clues about bond orientations and microscopic defect structures. A few centers in  $\beta$ -Ga<sub>2</sub>O<sub>3</sub> have been analyzed previously for D<sup>+</sup> implanted samples and for impurity-D complexes.<sup>36,38</sup>

Our Fe-doped  $\beta$ -Ga<sub>2</sub>O<sub>3</sub> sample with an (010) face shows many of the O-D lines reported for deuterium in  $\beta$ -Ga<sub>2</sub>O<sub>3</sub>. The spectra for this thick sample have a high signal to noise ratio making this an excellent sample for a study of the polarization properties of the O-D lines.

Spectra measured for different angles of an analyzing polarizer for the (010) Fe-doped sample and their analysis are given as Supplementary data (Figs. S1 and S2). Transition moment directions with respect to the [102] direction that have been determined are shown in Table I. The angles involved in this analysis are shown in Fig. S3.

(ii) Polarization with E//[010]: The transition moments for O-H and O-D vibrational modes observed experimentally for  $\beta$ -Ga<sub>2</sub>O<sub>3</sub> lie predominantly in the (010) plane, that is, there is no absorption observed with a component with polarization E//[010]. This result has led theory to propose structures with O-H trapped at split configurations of a Ga(1) vacancy.<sup>19</sup> O-H trapped at a vacancy at the Ga(2) site is predicted to have a transition moment with a component with E//[010] and thus had been ruled out.

Recently, O-D lines at 2475 and 2493 cm<sup>-1</sup> have been reported with a component of their transition moment along the [010] direction for the same Fe-doped,  $\beta$ -Ga<sub>2</sub>O<sub>3</sub> sample grown by the Czochralski method that is being studied here.<sup>39</sup> This led to the assignment of these lines to O-D trapped at a  $V_{Ga2}$  defect that could either be isolated or in the vicinity of another impurity.

Spectra are shown in Fig. 6 for a  $\beta$ -Ga<sub>2</sub>O<sub>3</sub>:Fe sample with a cleaved (100) face. The spectra that are shown have polarizations with **E**//[001] and **E**//[010|. This sample was deuterated with our usual 6 hr, 900°C, annealing treatment in a D<sub>2</sub> ambient followed by a subsequent anneal at 350°C to produce the additional lines seen for this narrow range of

This is the author's peer reviewed, accepted manuscript. However, the online version of record will be different from this version once it has been copyedited and typeset. PLEASE CITE THIS ARTICLE AS DOI: 10.1063/5.0160331

annealing temperatures. In addition to the lines at 2475 and 2493 cm<sup>-1</sup>, a line at 2467 cm<sup>-1</sup> with a component along [010] is also seen.

The spectra in Figs. 4 and 6 show that there is a group of lines that is thermally stable in the window of annealing temperatures near 350°C (2462, 2467, 2500, 2550, 2555, and 2560 cm<sup>-1</sup>), but of these, only the line at 2467 cm<sup>-1</sup> has a transition moment with a component along [010].

## D. Free-carrier absorption and the hydrogen passivation of $V_{Ga1}$

H has been predicted to act as an n-type dopant in  $\beta$ -Ga<sub>2</sub>O<sub>3</sub>,<sup>10</sup> and there have also been experimental reports of H introducing n-type conductivity.<sup>11,17</sup> In our experiments on the annealing of unintentionally doped  $\beta$ -Ga<sub>2</sub>O<sub>3</sub> hydrogenated by annealing in H<sub>2</sub> and D<sub>2</sub> ambients, we have also investigated the free-carrier absorption that hydrogen might give rise to. (Our Fedoped sample did not show any obvious hydrogen-related free-carrier absorption.)

A set of spectra that shows the broad absorption at low frequency that free carriers give rise to is presented in Fig. 7(a). This particular sample had been treated in a mixture of both D<sub>2</sub> and H<sub>2</sub> and also shows the O-D and O-H modes at 2546 and 3437 cm<sup>-1</sup> assigned to the  $V_{Ga1}^{ib}-2D$  and  $V_{Ga1}^{ib}-2H$  complexes.<sup>19</sup> The spectrum labeled "0" was measured for the sample immediately after a hydrogenation treatment. The other spectra are a selection of those measured following a series of sequential anneals in an inert Ar ambient at the temperatures shown. To produce a reference spectrum for a sample that did not contain H or D, this same sample was annealed in an Ar ambient at 1000°C for 4 hr, a treatment that was found to completely remove O-H and O-D IR lines from the sample. With such a hydrogen-free reference sample, the changes in the spectra shown in Fig. 7 are due to changes in the H or D in the sample.

The dashed line in Fig. 7(a) was measured for a Sn-doped  $\beta$ -Ga<sub>2</sub>O<sub>3</sub> wafer with a ( $\bar{2}01$ ) face whose n-type conductivity was characterized by Hall effect measurements to produce a calibration of the free-carrier absorption. This calibration sample had an n-type doping of N<sub>D</sub>-N<sub>A</sub> = 6.7 x10<sup>18</sup> cm<sup>-3</sup> and a mobility of 9 cm<sup>2</sup>/V-s. The free-carrier absorption shown for the dashed line in Fig. 10 yields the following approximate calibration for the free-carrier absorption coefficient ( $\alpha$ <sub>FC</sub>) measured at 2000 cm<sup>-1</sup>:

$$N_D - N_A = (5 \times 10^{16} \ cm^{-2}) \left[ \alpha_{FC} (2000 \ cm^{-1}) \right].$$
 (1)

## Applied Physics

This is the author's peer reviewed, accepted manuscript. However, the online version of record will be different from this version once it has been copyedited and typeset.

PLEASE CITE THIS ARTICLE AS DOI: 10.1063/5.0160331

The free-carrier absorption spectra in Fig. 7(a) show that the introduction of H and D into our unintentionally-doped sample increases the free-carrier absorption (spectrum "0"). Upon annealing in an inert ambient at successively higher temperatures, the free-carrier absorption increased steadily. If we compare these results for the free-carrier absorption in Fig. 7(a) with the annealing results for the O-D local modes shown in Figs. 1 and 2, we see that the increase in the free-carrier absorption depends on temperature in a way that is similar to the annealing behavior of the  $V_{Ga1}^{ib}-2D$  complex.

Fig. 7(b) shows an expansion of the spectral region where the O-H mode due to the  $V_{Ga1}^{ib}-2H$  center is seen. (The corresponding O-D mode seen for the same annealing sequence behaves similarly.) The increase in the free-carrier absorption and the local mode intensities in Figs. 7(a) and 7(b) mimic each other with a strong increase upon annealing at 500°C and a strong decrease at 1000°C when H and D are annealed away. Fig. 8 shows a plot for this set of anneals of the free carrier absorption coefficient at 2000 cm<sup>-1</sup> (left axis) that is proportional to the free carrier concentration vs. the integrated absorption coefficient for the O-H and O-D vibrational modes at 3447 and 2546 cm<sup>-1</sup> (lower axis).

The absorption coefficients for both the free carrier absorption and vibrational-mode absorption shown in Fig. 8 can be converted into approximate defect concentrations. The free-carrier absorption on the left axis is converted to the free-electron concentration on the right axis with the calibration given in Eq.(1). (Samples have been presumed to be n-type in the saturation regime with a free-electron concentration of n=N<sub>D</sub>-N<sub>A</sub> where any hole conductivity can be neglected.) The vibrational mode absorption on the lower axis is converted to the total concentration of H and D trapped in the form of  $V_{Ga1}^{ib} - 2H$  and  $V_{Ga1}^{ib} - 2D$  centers with Eq. (2)<sup>29</sup> and the calibration for these defects determined by Karjalainen *et al.*<sup>14</sup>

$$N = (2.303 \, nc^2 m) / (\pi q^2 d) \int A(\bar{v}) d\bar{v}. \tag{2}$$

Here,  $A(\bar{v})$ , is the absorbance as a function of frequency in wavenumber (cm<sup>-1</sup>) units, d is the thickness of the sample, m is the reduced mass of the oscillating impurity, c is the speed of light, and n is the refractive index. In this equation, the calibration is expressed as an effective charge, taken here to be q = 0.33e per H or D atom, that contributes to the absorption.

PLEASE CITE THIS ARTICLE AS DOI: 10.1063/5.0160331

## The absolute concentrations on the two axes in Fig. 8 differ only by a factor near 2 which is gratifying given the typical uncertainties in the independent calibrations that we have attempted. (The strength of the free-carrier absorption, for example, depends on the mobility of the charge carriers, $^{31,32}$ and the mobility for electrons in $\beta$ -Ga $_2$ O $_3$ is known to vary with the donor concentration. Furthermore, an uncertainty of a factor of 2 in a vibrational mode calibration is also typical unless great care is taken. <sup>29</sup>) IV. DISCUSSION A. Classes of O-D centers

Our IR spectra for O-D centers in unintentionally doped (Fig. 1) and Fe-doped  $\beta$ -Ga<sub>2</sub>O<sub>3</sub> (Figs. 4 and 6) show more than a dozen vibrational lines. These can be grouped into a few classes of defects based on their annealing and polarization properties. The different classes of O-D centers in  $\beta$ -Ga<sub>2</sub>O<sub>3</sub> and their regions of thermal stability are shown in Fig. 9. Transition moment directions (Table 1) for the different classes of defects are shown in Fig. S3(b).

- (i) There is the  $V_{Ga1}^{ib}-2D$  center that has been assigned to the 2546 cm<sup>-1</sup> line and is the dominant sink for D in undoped  $\beta$ -Ga<sub>2</sub>O<sub>3</sub> [black box in Fig. 9(a)]. Its isotope dependence and transition moment direction,  $\psi-X=15^\circ$  (clockwise with respect to [102]), are consistent with two identical D atoms bonded to a Ga vacancy with the split  $V_{Ga1}^{ib}$  configuration.<sup>19,43</sup>
- (ii) There is the group of O-D lines with frequencies between 2583 and 2631 cm<sup>-1</sup> (Fig. 1) that are introduced into unintentionally doped  $\beta$ -Ga<sub>2</sub>O<sub>3</sub> samples by an anneal in a D<sub>2</sub> ambient. These lines are eliminated together (Fig. 2) for an unintentionally doped sample by a subsequent anneal at 450°C in an inert ambient. Most of these lines have transition moment directions near  $\psi$  X = 90° (clockwise with respect to [102]) and are consistent with D bonded to a Ga(1) vacancy with the split  $V_{Ga1}^{ic}$  configuration [purple box in Fig. 9(a)]. Additional impurities or native defects are likely to be involved to explain the multiplicity of O-D modes that are seen.<sup>48</sup>
- (iii) Of the group of lines that are annealed away at 450°C, only the line at 2631 cm<sup>-1</sup> [green box in Fig. 9(a)] has polarization properties similar to those of the 2546 cm<sup>-1</sup> line suggesting that it may also involve D bonded to  $V_{Ga1}^{ib}$ . The 2631 cm<sup>-1</sup> center contains a single D atom<sup>21</sup> and perhaps an additional defect.
- (iv) The 2577 cm<sup>-1</sup> line seen for our Czochralski-grown, Fe-doped sample annealed in  $D_2$  [purple box in Fig. 9(b)] is the dominant O-D center and becomes a source of D in the sample

This is the author's peer reviewed, accepted manuscript. However, the online version of record will be different from this version once it has been copyedited and typeset PLEASE CITE THIS ARTICLE AS DOI: 10.1063/5.0160331

as it is annealed away (Fig 5). This line has polarization properties similar to those in group (ii), suggesting its assignment to an O-D centers involving a Ga(1) vacancy with the split  $V_{Ga1}^{ic}$  configuration and an additional impurity. The 2550 cm<sup>-1</sup> line has similar polarization properties suggesting a similar structure.

When the 2577 cm<sup>-1</sup> line is annealed away for this impurity-doped sample (Fig 5), the 2546 and 2631 cm<sup>-1</sup> centers become the dominant O-D defects [black and green boxes, respectively, in Fig. 9(b)].

- (v) There are 3 lines with a component of their polarization with  $\mathbf{E}$  // [010] [red box in Fig.9(b)]. These include the 2475 and 2493 cm<sup>-1</sup> lines (labeled in red in Fig. 6) that involve D trapped by a Ga(2) vacancy. The 2467 cm<sup>-1</sup> line also has a component with  $\mathbf{E}$  // [010] and appears only for a narrow range of post-deuteration annealing temperatures near 350°C
- (vi) There is a group of additional lines that appears only for a narrow window of post-deuteration annealing temperatures near 350°C. [Their labels (in blue) are underlined in Fig. 6.] The line at 2560 cm<sup>-1</sup> is a prominent example [blue box in Fig.9(b)] and has polarization properties similar to the 2546 and 2631 cm<sup>-1</sup> lines.

## B. $V_{Ga1}$ deep acceptors and their passivation by hydrogen

The annealing results for O-D centers in unintentionally doped  $\beta$ -Ga<sub>2</sub>O<sub>3</sub> presented in Fig. 2 and for the hydrogen-related free-carrier absorption presented in Fig. 8 provide information about how H and D in our experiments affect conductivity. Introducing D into a hydrogen-free sample by annealing in a D<sub>2</sub> ambient introduces the  $V_{Ga1}^{ib} - 2D$  center (2546 cm<sup>-1</sup> line) along with several weaker O-D lines with frequencies between 2583 to 2631 cm<sup>-1</sup> (Fig. 2). Similar hydrogen treatments also increase the absorption due to free carriers (Fig. 7, spectrum "0"). A subsequent anneal at 450°C in an inert ambient eliminates the weaker O-D centers and further increases the intensity of the 2546 cm<sup>-1</sup> line. For an anneal at the same temperature, Fig. 7 shows that the free-carrier absorption for a sample that contains H and D is also increased. Finally, an anneal at 1000°C in an inert ambient eliminates both the 2546 and 3437 cm<sup>-1</sup> lines and the free-carrier absorption related to hydrogen when D and H are presumed to leave the sample. Fig. 8 shows that the hydrogen-related free-carrier absorption is proportional to the vibrational absorption for  $V_{Ga1}^{ib} - 2H$  and  $V_{Ga1}^{ib} - 2D$  centers in the sample (see red line in the figure).

The results shown in Figs. 7 and 8 are consistent with the hydrogen passivation of  $V_{Ga1}$  triple acceptors that compensate unintentional shallow donors in the sample. That is,

This is the author's peer reviewed, accepted manuscript. However, the online version of record will be different from this version once it has been copyedited and typeset PLEASE CITE THIS ARTICLE AS DOI: 10.1063/5.0160331

when H or D become trapped by compensating  $V_{Ga1}$  centers to form (partially) passivated  $V_{Ga1}^{ib} - 2H$  or  $V_{Ga1}^{ib} - 2D$  complexes, both the free-carrier absorption and local mode intensities are increased together. These results are consistent with the conclusions of others who have proposed that the change in the n-type conductivity of  $\beta$ -Ga<sub>2</sub>O<sub>3</sub> upon annealing can be due to the introduction of compensating  $V_{Ga}$  deep acceptors.<sup>22</sup> Another study has suggested that the compensation of donors by  $V_{Ga}$  is strongly affected by the presence of H.<sup>14</sup>

H centers produced in β-Ga<sub>2</sub>O<sub>3</sub> by annealing in an H<sub>2</sub> ambient have been studied by others using DLTS and theory. In this case, annealing in an H<sub>2</sub> ambient produces the E1 DLTS peak whose broad width was suggested to be due to overlapping features. Theory considered whether different configurations of  $V_{Ga} - V_O$  centers complexed with H or impurity-H complexes might give rise to E1.<sup>21,48</sup> A broad DLTS peak due to overlapping features is reminiscent of our observation of several O-D vibrational lines with similar properties, causing us to consider whether similar hydrogen-containing centers might be involved in both DLTS and IR experiments.

## C. Theoretical analysis of V<sub>Ga(2)</sub>-nH centers

Figure 10 illustrates the structures of the unshifted Ga(2) vacancy and the Ga(2) - Ga(1) split vacancy, with primary H trapping sites shown. These structures share several properties. Each has one "axial" site whose O-H axis lies within the (010) plane, and two symmetry-equivalent "equatorial" sites whose O-H axes have (010) and [010] projections.

In Ref. [39] the vibrational lines at 2475 and 2493 cm<sup>-1</sup> were assigned to a single D trapped at an equatorial O(1) site at an unshifted Ga(2) vacancy, one line of which involved a neighboring substitutional Fe impurity. Each of these lines has an [010] projection along with an (010) component whose transition moment direction is in agreement with the computed result.

The additional lines reported in the present work have properties that are not as straightforward. Only the new line at 2467 cm<sup>-1</sup> has both an [010] projection and an (010) component; the others (e. g., 2462, 2500, 2560 cm<sup>-1</sup> and others) have no [010] component. Furthermore, several of these lines have similar thermal behavior; 2462, 2467, 2500, 2550, 2555, and 2560 cm<sup>-1</sup> appear around 350 °C and disappear again at higher T, while in the same temperature region the 2493 cm<sup>-1</sup> line weakens and then recovers. In addition, a 2484 cm<sup>-1</sup> line appears around 450 °C and then disappears at higher T.

This is the author's peer reviewed, accepted manuscript. However, the online version of record will be different from this version once it has been copyedited and typeset.

PLEASE CITE THIS ARTICLE AS DOI: 10.1063/5.0160331

## In an attempt to understand these results we have carried out a large number of calculations of the structures, energies, and vibrational frequencies of H trapped at candidate defects, using the CRYSTAL17 code<sup>51</sup> with parameters and basis functions as given in Ref. [39].

As noted in Ref. [39], we predict that the unshifted Ga(2) vacancy is energetically favored over the Ga(2) - Ga(1) split vacancy, by 0.34 eV. For a single trapped H, the lowest energy configuration is predicted to be H trapped on an equatorial O(1) at the unshifted Ga(2) vacancy, which in Ref. [39] was assigned to the 2475 cm<sup>-1</sup> line.

The next higher energy configuration, by 0.28 eV, is predicted to be the unshifted Ga(2) vacancy with H trapped on an axial O(2). This would not have an [010] projection. Its predicted anharmonic frequency is 22 cm<sup>-1</sup> lower than that of the H trapped on an equatorial O(1) and its transition moment would lie 132 degrees from [102].

The Ga (2) – Ga(1) split vacancy with H trapped on an equatorial O(2) with a transition moment in both [010] and (010) is predicted to lie 0.43 eV above that of H trapped on an equatorial O(1) at the unshifted Ga(2) vacancy configuration. Its predicted frequency is 18 cm<sup>-1</sup> lower than that of the unshifted case and its transition moment in (010) would lie 110 degrees from [102].

Turning to the unshifted Ga(2) vacancy with two trapped H, as noted in Ref. [39], two trapped H on the two equatorial O(1) sites would lead to one line in (010) and another in [010]. Since no line with only a [010] moment has been observed, this structure is not a candidate to interpret the present data. A similar comment holds for the split configuration.

However, one H trapped on an axial O(2) and a second trapped on an equatorial O(1) at the unshifted Ga(2) vacancy will yield one line with both [010] and (010) moments and a second line with no [010] projection. This configuration is predicted to lie only 0.05 eV higher than two H trapped on the two equatorial O(1), so these two configurations are essentially degenerate. In this case the line with a [010] projection is predicted to lie 3 cm<sup>-1</sup> lower than that of the single trapped H on an equatorial O(1). The line without a [010] projection is predicted to lie 20 cm<sup>-1</sup> higher than that of the single trapped H with a transition moment 134 degrees from [102].

Table II lists the relative energies of several of the configurations discussed here. Additional configurations with Fe or Ir neighbors and with three H have also been considered. Some may be rejected while others have properties not substantially different from those described above, so they could also be candidates.

PLEASE CITE THIS ARTICLE AS DOI: 10.1063/5.0160331

There is no obvious single defect configuration that could explain all of the lines that appear and then disappear around 350 °C. If we consider the two-H configuration of one axial and one equatorial, with the equatorial configuration responsible for the 2467 cm<sup>-1</sup> line, then the predicted axial line 20 cm<sup>-1</sup> higher could perhaps correspond to the 2500 cm<sup>-1</sup> line.

It seems likely that this cluster of lines represents several distinct defects that involve the Ga(2) vacancy, whose presence is created by their being "fed" by the 2493 cm<sup>-1</sup> defect, or even from the 2577 cm<sup>-1</sup> defect, which is extremely strong in these samples. They might, for example, be impurity- or oxygen-vacancy-related Ga(2) vacancies.

## D. Conversions between classes of O-D centers in β-Ga<sub>2</sub>O<sub>3</sub>

(i)  $V_{Ga1}^{ib}-2D$  and its formation in unintentionally doped β-Ga<sub>2</sub>O<sub>3</sub>: Our results in Figs. 1 and 2 show that all the D-containing centers in our unintentionally doped β-Ga<sub>2</sub>O<sub>3</sub> sample are converted into the  $V_{Ga1}^{ib}-2D$  center by an anneal at a temperature near 450°C.  $V_{Ga1}^{ib}-2D$  is then stable up to an annealing temperature of 1000°C. A puzzle that remains concerns the identity of the weak O-D lines between 2583 and 2631 cm<sup>-1</sup> and a mechanism for their evolution to the dominant 2546 cm<sup>-1</sup> line that occurs upon annealing at 450°C (Fig. 2). The defects giving rise to these weaker lines do not appear to result in the passivation of  $V_{Ga1}$  deep acceptors until their conversion to the  $V_{Ga1}^{ib}-2D$  center. A corresponding theoretical puzzle regarding these lines arises from the theoretical prediction that for structures with a single H (D) trapped at a relaxed  $V_{Ga1}$  center with the split "c" configuration, their vibrational frequencies should be lower than that of the primary 2546 cm<sup>-1</sup> line rather than higher.

A simple mechanism for the passivation of deep acceptors upon annealing could involve the presence of  $D_2$  or some other IR inactive defect that could act as a source for additional D. A reaction like,

$$2(V_{Ga1}^{ic} - D) + D_2 \to 2(V_{Ga1}^{ib} - 2D),$$
 (3)

could explain the elimination of  $V_{Ga1}^{ic}-D$  deep acceptors that results from the formation of passivated  $V_{Ga1}^{ib}-2D$  complexes upon annealing. A similar reaction might also explain the conversion of the 2631 cm<sup>-1</sup> center to the  $V_{Ga1}^{ib}-2D$  complex upon annealing at 450°C. Others have also suggested the presence of an IR inactive source of hydrogen in  $\beta$ -Ga<sub>2</sub>O<sub>3</sub> such as the hydrogen molecule.<sup>14</sup>

PLEASE CITE THIS ARTICLE AS DOI: 10.1063/5.0160331

(ii) Fe-doped  $\beta$ -Ga<sub>2</sub>O<sub>3</sub>: Contrasting the annealing behaviors of defects in Figs. 1 and 2 with those seen in Figs. 4 and 5 shows the effect that impurities such as Fe, Ir and Si with high concentration can have on the trapping of H or D in the sample. In the heavily Fe-doped, Czochralski-grown sample, the 2577 cm<sup>-1</sup> line is dominant throughout the annealing sequence. The 2546 cm<sup>-1</sup> line assigned to  $V_{Ga1}^{ib}-2D$  that was dominant in unintentionally doped samples is now a minority species and appears only after annealing.  $V_{Ga1}^{ib}-2D$  becomes a dominant defect in this sample only after metal-impurity-related lines are annealed away. The 2577 cm<sup>-1</sup> center is the dominant reservoir for D in our heavily impurity-doped samples, and it is this 2577 cm<sup>-1</sup> defect that feeds other D-containing centers upon annealing.

## V. CONCLUSION

Deuterium has been introduced into unintentionally-doped and Fe-doped  $\beta$ -Ga<sub>2</sub>O<sub>3</sub> samples by annealing in a D<sub>2</sub> ambient at elevated temperature to study the properties of the various classes of O-D centers that form, their evolution upon annealing, and their effect on conductivity. The angle dependence of polarized O-D vibrational absorption provides information about the orientations of the O-D bonds and clues about possible defect structures.

The  $V_{Ga1}^{ib}-2D$  center whose vibrational line is observed at 2546 cm<sup>-1</sup> is the dominant sink for D in unintentionally doped samples. Furthermore, a study of the free-carrier absorption in samples that were deuterated and annealed shows that the formation of this defect passivates the deep  $V_{Ga1}^{ib}$  triple acceptor and increases n-type conductivity by reducing the compensation of unintentional shallow donors.

Several additional O-D centers were produced by annealing treatments in  $D_2$ , several of which have a  $V_{Ga1}^{ic} - nD$  structure; the involvement of an additional defect could explain the existence of several O-D centers with similar properties. These O-D centers are converted into the dominant  $V_{Ga1}^{ib} - 2D$  defect by an anneal in an inert ambient at temperatures near 450°C. This reaction affects the n-type conductivity by further increasing the passivation of  $V_{Ga1}^{ib}$  triple acceptors. The microscopic nature of this reaction is not well understood and might possibly involve the release of D from a defect not seen by IR spectroscopy that then contributes to the passivation of  $V_{Ga1}$  deep acceptors.

The introduction of a high concentration of an impurity like Fe in  $\beta$ -Ga<sub>2</sub>O<sub>3</sub> gives rise to deep-level defects that effectively compete with  $V_{Ga1}$  centers for D. In a Czochralski-grown sample

PLEASE CITE THIS ARTICLE AS DOI: 10.1063/5.0160331

that had been doped with a high concentration of Fe, the  $V_{Ga1}^{ib}-2D$  became the dominant trap for D only after a strong O-D line at 2577 cm<sup>-1</sup> that is attributed to an OD-impurity complex had been annealed away.

O-D centers in  $\beta$ -Ga<sub>2</sub>O<sub>3</sub> with D trapped by the  $V_{Ga1}^{ib}$  or  $V_{Ga1}^{ic}$  defects all have a transition moment that lies in the (010) plane and show no vibrational absorption for the polarization with  $\mathbf{E}$ //[010]. While split  $V_{Ga1}$  centers are the dominant traps for D in our samples, the Czochralski-grown  $\beta$ -Ga<sub>2</sub>O<sub>3</sub> sample that contained a high concentration of Ir and Fe impurities showed additional O-D centers with surprising polarization properties. A few O-D centers have been observed with transition moments with a component with  $\mathbf{E}$ //[010] and assigned to defects with D trapped by a Ga(2) vacancy. Defects involving both an unshifted  $V_{Ga2}$  configuration and a split vacancy configuration ( $V_{Ga1}^{ia}$ ) that includes  $V_{Ga1}$  and  $V_{Ga2}$  half vacancies have been considered.

While the large number of O-D centers seen in our experiments and those of others suggests that hydrogen's effect on the conductivity of  $\beta$ -Ga<sub>2</sub>O<sub>3</sub> will be complex, some general behaviors involving the interaction of D with  $V_{Ga}$  deep acceptors that compensate the n-type conductivity of Ga<sub>2</sub>O<sub>3</sub> have been observed. Nonetheless, much work remains to be done to understand the microscopic mechanisms for the hydrogen-related reactions that occur even for the relatively simple case where H or D is introduced into  $\beta$ -Ga<sub>2</sub>O<sub>3</sub> by annealing in an H<sub>2</sub> or D<sub>2</sub> ambient.

## SUPPLEMENTARY MATERIAL

See the supplementary material for spectroscopic data and its analysis for the polarization dependence of the O-D vibrational modes introduced into  $\beta$ -Ga<sub>2</sub>O<sub>3</sub> by an annealing treatment in a D<sub>2</sub> ambient at 900°C.

## **ACKNOWLEDGEMENTS**

The 1 cm thick  $\beta$ -Ga<sub>2</sub>O<sub>3</sub> sample studied here was grown by the Czochralski method at Synoptics. The work at Lehigh University was supported by NSF Grant No. DMR 1901563 (James Edgar). The work at UF was sponsored by Department of the Defense, Defense Threat Reduction Agency, HDTRA1-17-1-011, monitored by J. Calkins, DTRA Interaction of Ionizing Radiation with Matter University Research Alliance, HDTRA1-19-S-0004 (Jacob Calkins) and

This is the author's peer reviewed, accepted manuscript. However, the online version of record will be different from this version once it has been copyedited and typeset.

PLEASE CITE THIS ARTICLE AS DOI: 10.1063/5.0160331

also by NSF DMR 1856662 (James Edgar). Portions of this research were conducted on Research Computing resources provided by Lehigh University supported by the NSF award 2019035. E.R. Glaser acknowledges the support of the Office of Naval Research.

## Conflicts of Interest

The authors have no conflicts to disclose.

## DATA AVAILABILITY

The data that support the findings of this study are available from the corresponding author upon reasonable request.

on of record will be different from this version once it has been copyedited and typeset. PLEASE CITE THIS ARTICLE AS D This is the author's peer reviewed, accepted manuscript. However, the online versi

Table I. Frequencies (77 K) of O-D IR lines seen for an Fe-doped  $\beta$ -Ga<sub>2</sub>O<sub>3</sub> sample that had been deuterated by annealing in a D<sub>2</sub> ambient (6 hr, 900 °C). (The lines shown in bold italics were seen only for our Fe-doped sample grown by the Czochralski method. Lines shown in regular typeface were also seen for an unintentionally doped sample.) The absolute value of the angle X of the transition moment with respect to the X dielectric axis is shown. The angle  $\Psi \pm X$  gives the transition moment direction measured clockwise with respect to the [102] crystal axis. Transition moment directions that agree with values determined by theory for predicted structures are shown in bold-face type.

ω <sub>D</sub> (cm <sup>-1</sup> )	2475	2493	2550	2560	2577	2583	2592	2602	2611	2620	2631
X   X	$22^{o+13}_{-22}$	$26^{o+6}_{-13}$	63° ± 4	39°+4	62° ± 1	58° ± 3	59° ± 2	51° ± 2	$51^{o+8}_{-10}$	53° ± 2	36° ± 2
$\psi -  X $	14°+26	10°+17	$-27^{\circ} \pm 8$	-3°+9	$-26^{\circ} \pm 5$	$-22^{\circ} \pm 7$	-23° ± 6	$-15^{\circ} \pm 6$	$-15^{\circ +14}_{-12}$	−17° ± 6	0° ± 6
- 01 ψ +  X	58°+17	62°+10	99° ± 8	75°+8	98° ± 5	94° ± 7	95° ± 6	87° ± 6	87°+12	$88^{\circ} \pm 6$	72° ± 6

Table II. Computed Ga(2) vacancy and Ga(2)-Ga(1) split vacancy  $(V^{ia}_{\it Ga})$  relative energies.

Defect and charge state	ΔE (eV)					
Bare vacancy (-3)						
Unshifted	0.00					
Split vacancy	0.34					
Vacancy plus one H (-2)						
H on equatorial O(1)	0.00					
H on axial O(2)	0.28					
Split vacancy, H on equatorial O(2)	0.43					
H on axial O(3)	0.49					
Split vacancy, H on axial O(2)	0.92					
Vacancy plus two H (-1)						
H's on equatorial O(1)	0.00					
H on equatorial O(1), H on axial O(2)	0.05					
Split vacancy, H's on equatorial O(2)	0.32					

This is the author's peer reviewed, accepted manuscript. However, the online version of record will be different from this version once it has been copyedited and typeset. PLEASE CITE THIS ARTICLE AS DOI: 10.1063/5.0160331

## REFERENCES

- 1. *Ultrawide bandgap* β-Ga<sub>2</sub>O<sub>3</sub> *semiconductor: Theory and applications*, edited by J. S. Speck and E. Farzana (AIP Publishing, Melville, NY, 2023).
- 2. *Gallium oxide: Materials properties, crystal growth, and devices*, edited by M. Higashiwaki and S. Fujita (Springer, Switzerland, 2020).
- 3. J. Zhang, P. Dong, K. Dang, Y. Zhang, Q. Yan, H. Xiang, J. Su, Z. Liu, M. Si, J. Gao, M. Kong, H. Zhou and Y. Hao, Nat. Commun. 13, 3900 (2022).
- 4. S. J. Pearton, J. Yang, P. H. Cary, F. Ren, J. Kim, M. J. Tadjer, and M. A. Mastro, Appl. Phys. Rev., **5**, 011301 (2018).
- 5. M. Higashiwaki, A. Kuramata, H. Murakami, and Y. Kumagai, J. Phys. D: Appl. Phys., **50**, 333002 (2017).
- 6. M. D. McCluskey, J. Appl. Phys. 127, 101101 (2020).
- 7. P. D. C. King and T. D. Veal, J. Phys. Condens. Matter, 23, 334214 (2011).
- 8. M. D. McCluskey, M. C. Tarun, and S. T. Teklemichael, J. Mater. Res., 17, 2190 (2012).
- 9. M. Stavola, W. B. Fowler, Y. Qin, P. Weiser, and S. J. Pearton, in *Ga*<sub>2</sub>*O*<sub>3</sub>, *Technology*, *Devices and Applications*, S. J. Pearton, F. Ren, and M. Mastro, Editors, Chapter 9, p. 191, Elsevier, Amsterdam (2018).
- 10. J. B. Varley, J. R. Weber, A. Janotti, and C. G. Van de Walle, Appl. Phys. Lett., **97**, 142106 (2010).
- 11. M. M. Islam, M. O. Liedke, d. Winarski, M. Butterling, A. Wagner, P. Hoseman, Y. Wang, B. Uberuaga, and F. A. Selim, Scientific Reports **10**, 6134 (2020).
- 12. M. E. Ingebrigtsen, J. B. Varley, A. Yu Kuznetsov, B. G. Svensson, G. Alfieri, M. Mihaila, J. Badstübner, and L. Vines, Appl. Phys. Lett **112**, 042104 (2018).
- 13. A. Portoff, A. Venzie, Y. Qin, M. Stavola, W. B. Fowler, and S. J. Pearton, ECS J. Solid State Sci. Technol. **9**, 125006 (2020).
- 14. A. Karjalainen, P. M. Weiser, I. Makkonen, V. Reinertsen, L. Vines, F. Tuomisto, J. Appl. Phys. **129**, 165702 (2021).
- 15. A. Y. Polyakov, I.-H. Lee, N. B. Smirnov, E. B. Yakimov, I. V. Shchemerov, A. V. Chernykh, A. I. Kochkova, A. A. Vasilev, A. S. Shiko, F. Ren, P. H. Carey, and S. J. Pearton, Appl. Phys. Lett. **115**, 032101 (2019).
- A. Y. Polyakov, I.-H. Lee, N. B. Smirnov, E. B. Yakimov, I. V. Shchemerov, A. V. Chernykh,
   A. I. Kochkova, A. A. Vasilev, A. S. Shiko, P. H. Carey, F. Ren, and S. J. Pearton, ECS J.
   Solid State Sci. Technol. 8, P661 (2019).

## the online version of record will be different from this version once it has been copyedited and typeset This is the author's peer reviewed, accepted manuscript. However, the online version of record will be diff PLEASE CITE THIS ARTICLE AS DOI: 10.1063/5.0160331

- 17. A. Y. Polyakov, I.-H. Lee, A. Miakonkikh, A. V. Chernykh, N. B. Smirnov, I. V. Shchemerov, A. I. Kochkova, A. A. Vasilev, and S. J. Pearton, J. Appl. Phys. **127**, 175702 (2020)
- 18. Q. Jiang, J. Meng, Y. Shi, Z. Yin, J. Chen, J. Zhang, J. Wu, and X. Zhang, J. Semicond. **43**, 092802 (2022).
- 19. P. Weiser, M. Stavola, W. B. Fowler, Y. Qin, Appl. Phys. Lett. 112, 232104 (2018).
- 20. Y. Qin, M. Stavola, W. B. Fowler, P. Weiser, and S. J. Pearton, ECS J. Solid State Sci. Technol. **8**, Q3103 (2019).
- 21. A. Langørgen, C. Zimmermann, Y. K. Frodason, E. F. Verhoeven, P. M. Weiser, R. M. Karsthof, J. B. Varley, and L. Vines, J. Appl. Phys. **131**, 115702 (2022).
- 22. J. B. Varley, H. Peelaers, A. Janotti, and C. G. Van de Walle, J. Phys.: Condens. Matter **23**, 334212 (2011).
- 23. A. Krytsos, M. Matsubara, and E. Bellotti, Phys. Rev. B 95, 245202 (2017).
- 24. J. B. Varley, in *Gallium oxide: Materials properties, crystal growth, and devices*, Ref. 2, Chapt. 18, p. 329.
- 25. H. J. von Bardeleben, S. Zhou, U. Gerstmann, D. Skachkov, W. R. L. Lambrecht, Q. Ho, and P. Deak, APL Mater. **7**, 022521 (2019).
- 26. D. Skachkov, W. R. L. Lambrecht, H. J. von Bardeleben, U. Gerstmann, Q. D. Ho, and P. Deák, J. Appl. Phys. **125**, 185701 (2019).
- 27. J. M. Johnson, Z. Chen, J. B. Varley, C. M. Jackson, E. Farzana, Z. Zhang, A. R. Arehart, H.-L. Huang, A. Genc, S. A. Ringel, C. G. Van de Walle, D. A. Muller, and J. Hwang, Phys. Rev. **X9**, 041027 (2019).
- 28. A. Karjalainen, V. Prozheeva, K. Simula, I. Makkonen, V. Callewaert, J. B. Varley, and F. Tuomisto, Phys. Rev. B **102**, 195207 (2020).
- 29. M. Stavola, in *Identification of Defects in Semiconductors*, ed. M. Stavola (Academic, Boston, 1998), Vol. 51B, Chap. 3, p. 153.
- 30. M. Stavola and W. B. Fowler, J. Appl. Phys. 123, 161561 (2018).
- 31. H. Y. Fan, in *Optical Properties of III-V Compounds*, R.K. Willardson and A.C. Beer, Editors, Chapter 9, p. 405, Academic, New York (1967).
- 32. D. K. Schroder, R. N. Thomas, and J. C. Swartz, <u>IEEE Trans. Electron Devices</u> **25**, 254 (1978).
- 33. A. Y. Polyakov, N. B. Smirnov, I. V. Shchemerov, S. J. Pearton, F. Ren, A. V. Chernykh, and A. I. Kochkova, Appl. Phys. Lett. **113**, 142102 (2018).
- 34. J. R. Ritter, K. G. Lynn, and M. D. McCluskey, J. Appl. Phys. 126, 225706 (2019)
- 35. J. R. Ritter, K. G. Lynn, and M. D. McCluskey, Proc. SPIE 10919, 109190Z (2019).

- This is the author's peer reviewed, accepted manuscript. However, the online version of record will be different from this version once it has been copyedited and typeset. PLEASE CITE THIS ARTICLE AS DOI: 10.1063/5.0160331
- 36. A. Venzie, A. Portoff, E. C. Perez Valenzuela, M. Stavola, W. B. Fowler, S. J. Pearton, and E. R. Glaser, J. Appl. Phys. **131**, 035706 (2022).
- 37. Z. Galazka, J. Appl. Phys. 131, 031103 (2022).
- 38. A. Portoff, A. Venzie, Y. Qin, M. Stavola, W. B. Fowler, and S. J. Pearton, ECS J. Solid State Sci. Technol. **9**, 125006 (2020).
- 39. A. Portoff, M. Stavola, W. B. Fowler, S. J. Pearton, and E. R. Glaser, Appl. Phys. Lett. **122**, 062101 (2023).
- 40. S. Geller, J. Chem. Phys. 33, 676 (1960).
- 41. J. Åhman, G. Svensson, and J. Albertsson, Acta Cryst., C52, 1336 (1996).
- 42. C. Sturm, J. Furthmüller, F. Bechstedt, R. Schmidt-Grund, and M. Grundmann, APL Materials **3**, 106106 (2015).
- 43. A. Portoff, A. Venzie, M. Stavola, W. B. Fowler, and S. Pearton, J. Appl. Phys. **127**, 055702 (2020).
- 44. EAG Laboratories, https://www.eag.com/techniques/mass-spec/secondary-ion-mass-spectrometry-sims/
- 45. E. G. Villora, K. Shimamura, Y. Koshikawa, T. Ujiie, and K. Aoki, Appl. Phys. Lett. **92**, 202120 (2008).
- 46. A. Venzie, A. Portoff, C. Fares, M. Stavola, W. B. Fowler, F. Ren, and S. J. Pearton, Appl. Phys. Lett. **119**, 062109 (2021).
- 47. K. Sasaki, S. Yamakoshi, and A. Kuramata, in *Gallium oxide: Materials properties, crystal growth, and devices*, Ref. 2, Chapt. 7, Fig. 7.18.
- 48. A. Langørgen, C. Zimmermann, Y. K. Frodason, E. F. Verhoeven, P. M. Weiser, R. M. Karsthof, J. B. Varley, and L. Vines, J. Appl. Phys. **131**, 115702 (2022).
- 49. P. Ugliengo, see http://www.moldraw.unito.it for "MOLDRAW" (2006).
- 50. See http://povray.org for "POV-Ray."
- 51. R. Dovesi, A. Erba, R. Orlando, C.M. Zicovich-Wilson, B. Civalleri, L. Maschio, M. R´erat, S. Casassa, J. Baima, S. Salustro, B. Kirtman, WIREs Comput. Mol. Sci., e1360 (2018)
  Quantum-Mechanical Condensed Matter Simulations with CRYSTAL.

This is the author's peer reviewed, accepted manuscript. However, the online version of record will be different from this version once it has been copyedited and typeset. PLEASE CITE THIS ARTICLE AS DOI: 10.1063/5.0160331

## Figure captions

Fig. 1. Polarized IR absorption spectra (77 K, resolution 1 cm<sup>-1</sup>) for an undoped ( $\bar{2}01$ )  $\beta$ -Ga<sub>2</sub>O<sub>3</sub> sample annealed in a D<sub>2</sub> ambient at 900°C. The propagation vector of the incident light had a 45° angle with respect to the ( $\bar{2}01$ ) face of the sample. The sample was sequentially annealed at the temperatures shown (°C) in a flowing Ar ambient.

Fig. 2. Panels (a) and (b) show the integrated absorbances for the IR lines with the given frequencies vs annealing temperature. (The frequency and corresponding data for a representative defect are shown along with the frequencies, in parentheses, for lines that show similar annealing behavior.) Anneals (30 min) were performed in a flowing Ar ambient. "0" corresponds to the as-deuterated sample. Lines are drawn to guide the eye.

Fig. 3. SIMS concentration profiles for Fe, Ir, Mg and Si impurities in a  $\beta$ -Ga<sub>2</sub>O<sub>3</sub> boule grown by the Czochralski method that had been intentionally doped with Fe. The detection limits for Fe, Mg and Si are 5 x 10<sup>14</sup>, 1 x 10<sup>14</sup> and 5 x 10<sup>14</sup> cm<sup>-3</sup> respectively.<sup>44</sup>

Fig. 4. Panels (a) and (b) show polarized IR absorption spectra (77 K, resolution 1 cm<sup>-1</sup>) for an  $(010) \, \beta$ -Ga<sub>2</sub>O<sub>3</sub> boule grown by the Czochralski method that had been doped with Fe. This sample was annealed in a D<sub>2</sub> ambient at 900°C to introduce D and was then sequentially annealed at the temperatures shown (°C) in a flowing Ar ambient. "0" corresponds to the asdeuterated sample.

Fig. 5. Panels (a), (b), and (c) show integrated absorbances for the IR lines with the given frequencies vs. annealing temperature for the Czochralski-grown, Fe-doped  $\beta$ -Ga<sub>2</sub>O<sub>3</sub> sample whose spectra are shown in Fig. 4. Anneals (30 min) were performed in a flowing Ar ambient. Lines are drawn to guide the eye. Panel (c) lists a group of lines in parentheses with annealing dependences similar to those shown.

Fig. 6. Polarized IR absorption spectra (77K, resolution 1 cm<sup>-1</sup>) for an Fe-doped  $\beta$ -Ga<sub>2</sub>O<sub>3</sub> boule annealed in a D<sub>2</sub> ambient at 900°C. The sample was subsequently annealed for 30 min at 350°C in a flowing Ar ambient. (The "blue underlined frequencies were only observed for an annealing temperature near 350°C.) Vibrational absorption is compared for the polarizations E//[001] (upper spectrum) and E//[010] (lower spectrum).

## This is the author's peer reviewed, accepted manuscript. However, the online version of record will be different from this version once it has been copyedited and typeset PLEASE CITE THIS ARTICLE AS DOI: 10.1063/5.0160331

Fig. 7. (a) Selection of free-carrier absorption spectra (77 K, resolution 1 cm<sup>-1</sup>) measured for an undoped β-Ga<sub>2</sub>O<sub>3</sub> sample that had first been annealed in a mixture of H<sub>2</sub> and D<sub>2</sub> (900°C, 8h). The sample was subsequently annealed (30 min) in Ar gas at the temperatures shown. The reference spectrum (not shown) was measured for the sample after an anneal at 1000°C (4 h) to remove H and D. The free-carrier absorption spectrum shown dashed (blue curve) was measured for a Sn-doped β-Ga<sub>2</sub>O<sub>3</sub> sample whose carrier concentration was determined by Hall effect measurements. The free-carrier absorption spectra have been off-set vertically to give a common zero at 4000 cm<sup>-1</sup> where the absorbance becomes approximately constant. (b) The IR line at 3437 cm<sup>-1</sup> due to the  $V_{Ga1}^{ib} - 2H$  center that is also shown in panel (a). These expanded spectra have been baseline corrected to remove the effect of free-carriers and off-set vertically for clarity.

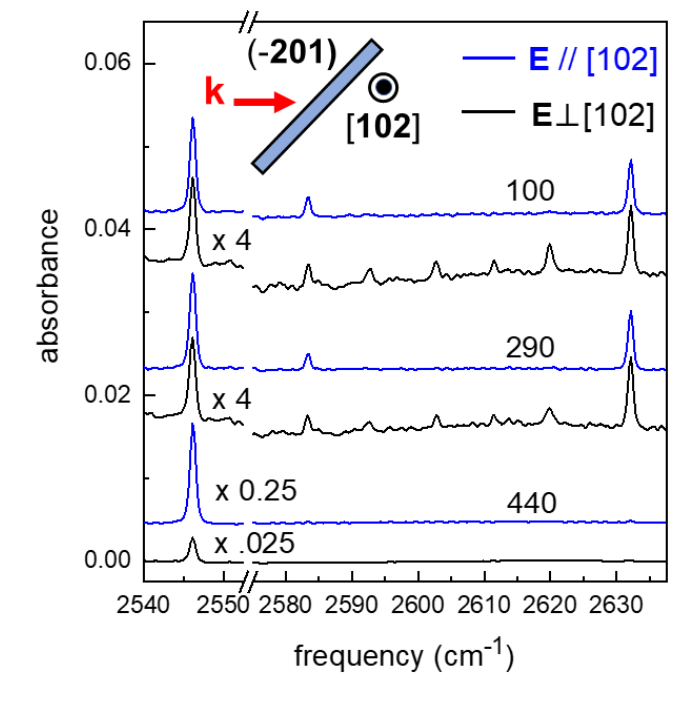
Fig. 8. Free-carrier absorption vs local vibrational mode absorption for an undoped β-Ga<sub>2</sub>O<sub>3</sub> sample containing H and D following various annealing treatments. The left axis shows the absorption coefficient measured at 2000 cm<sup>-1</sup> arising from free carriers. The bottom axis shows the sum of the integrated absorption coefficients for the O-H and O-D vibrational modes assigned to  $V_{Ga1}^{ib} - 2H$  and  $V_{Ga1}^{ib} - 2D$  complexes weighted by the ratio of the masses of the oscillating H or D atoms. The concentration of free carriers, N<sub>D</sub>-N<sub>A</sub>, (right axis) and the concentration of H plus D (trapped in the form of  $V_{Ga1}^{ib} - 2H$  and  $V_{Ga1}^{ib} - 2D$  centers) (top axis) determined from approximate calibrations of the free-carrier absorption and integrated-vibrational-mode absorption, respectively.

Fig. 9. Different classes of O-D centers and their regions of thermal stability in (a) unintentionally-doped β-Ga<sub>2</sub>O<sub>3</sub> and (b) Fe-doped, Czochralski-grown β-Ga<sub>2</sub>O<sub>3</sub>.

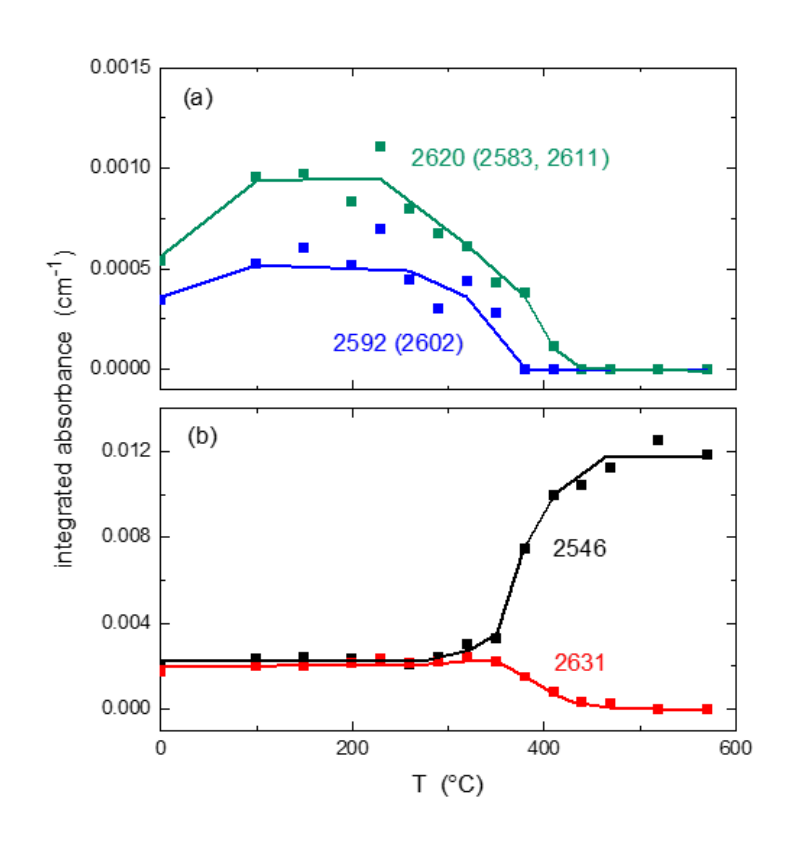
Fig. 10. Primary H trapping sites at (a) the unshifted Ga(2) vacancy and (b) the split Ga(2) vacancy – Ga – Ga(1) vacancy. In each case one O-H direction lies within the (010) plane while two, symmetry-equivalent, directions have components within the (010) plane and in the [010] direction. Atoms are color coded as follows: Ga(1), purple; Ga(2), dark green; O(1), red; O(2), yellow; O(3), light green; H sites, blue; Ga(2) site, gray. Crystalline directions are noted. This figure was constructed using MOLDRAW<sup>49</sup> and POV-Ray<sup>50</sup>.

This is the author's peer reviewed, accepted manuscript. However, the online version of record will be different from this version once it has been copyedited and typeset.

PLEASE CITE THIS ARTICLE AS DOI: 10.1063/5.0160331



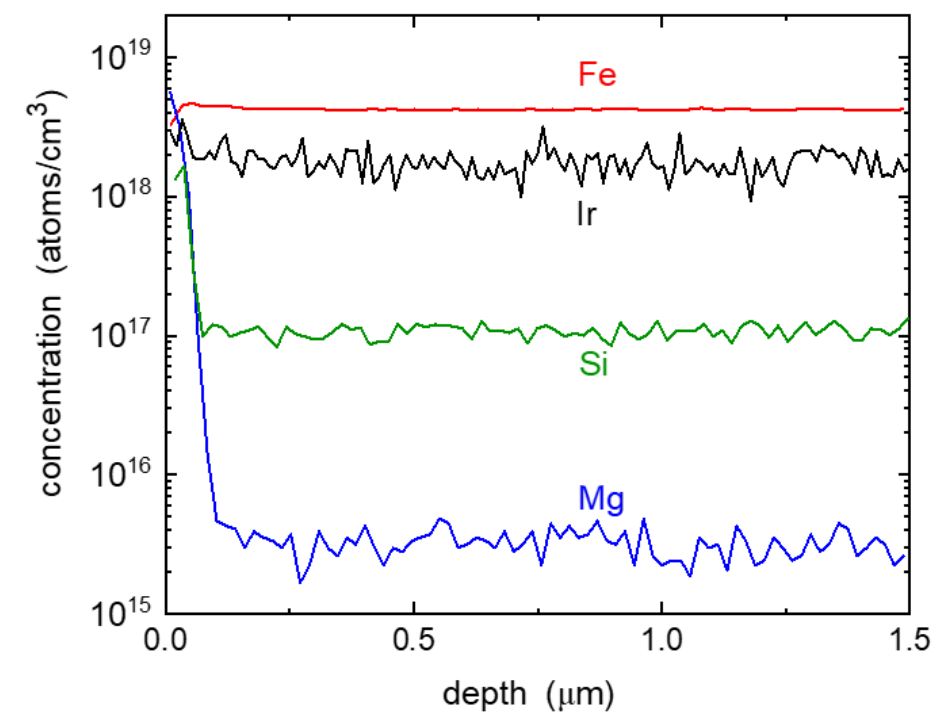
F1



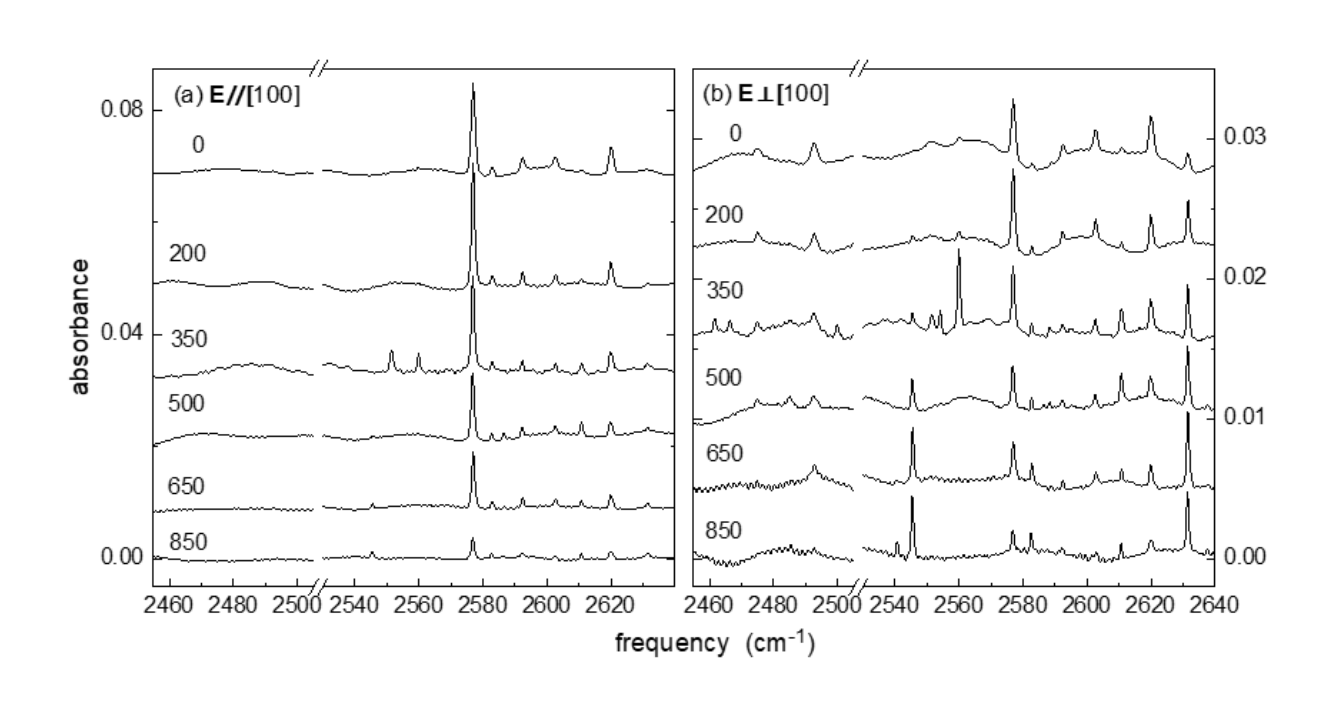
## **Applied Physics**

This is the author's peer reviewed, accepted manuscript. However, the online version of record will be different from this version once it has been copyedited and typeset.

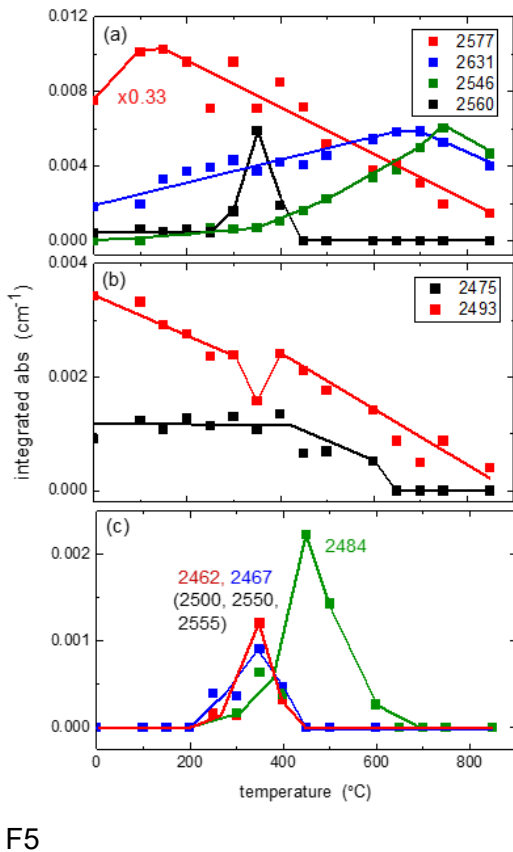


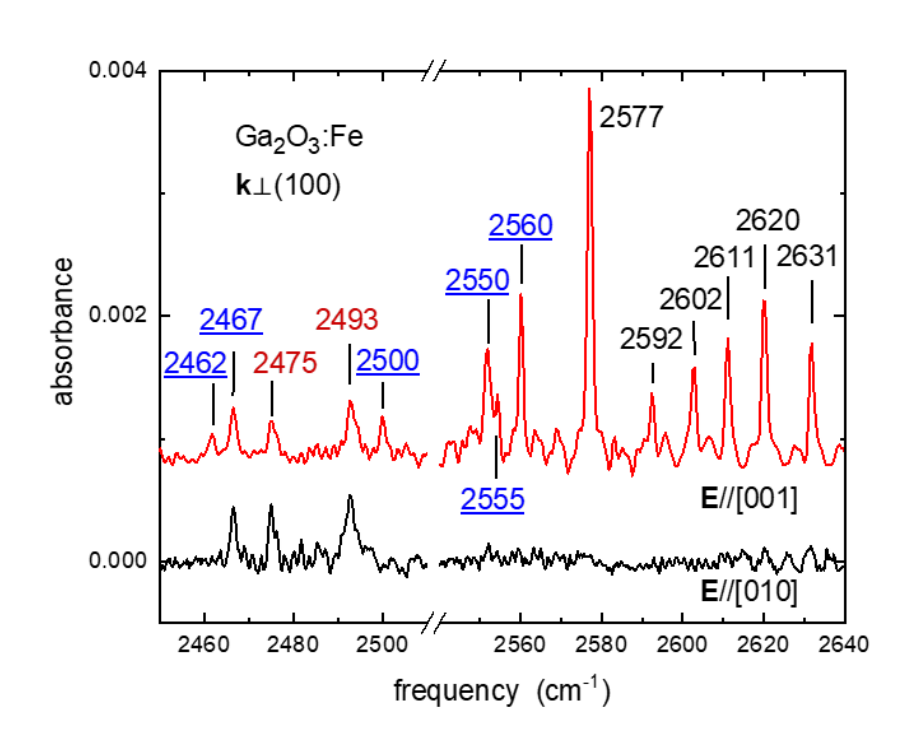


F3



PLEASE CITE THIS ARTICLE AS DOI: 10.1063/5.0160331

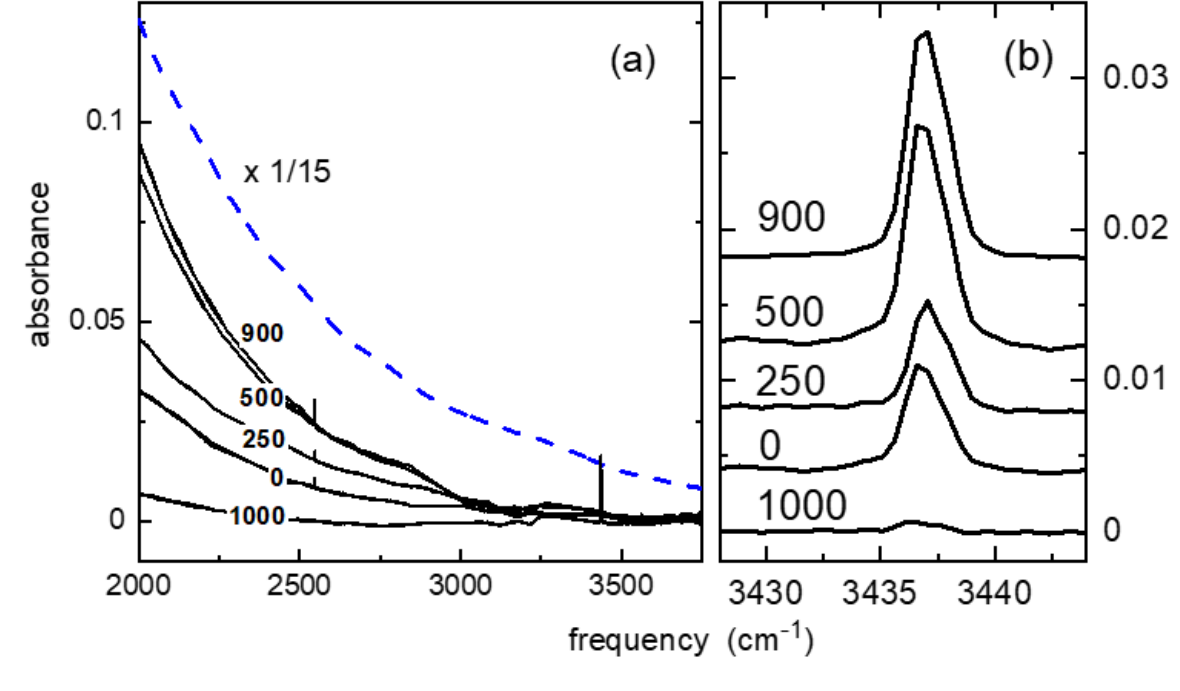




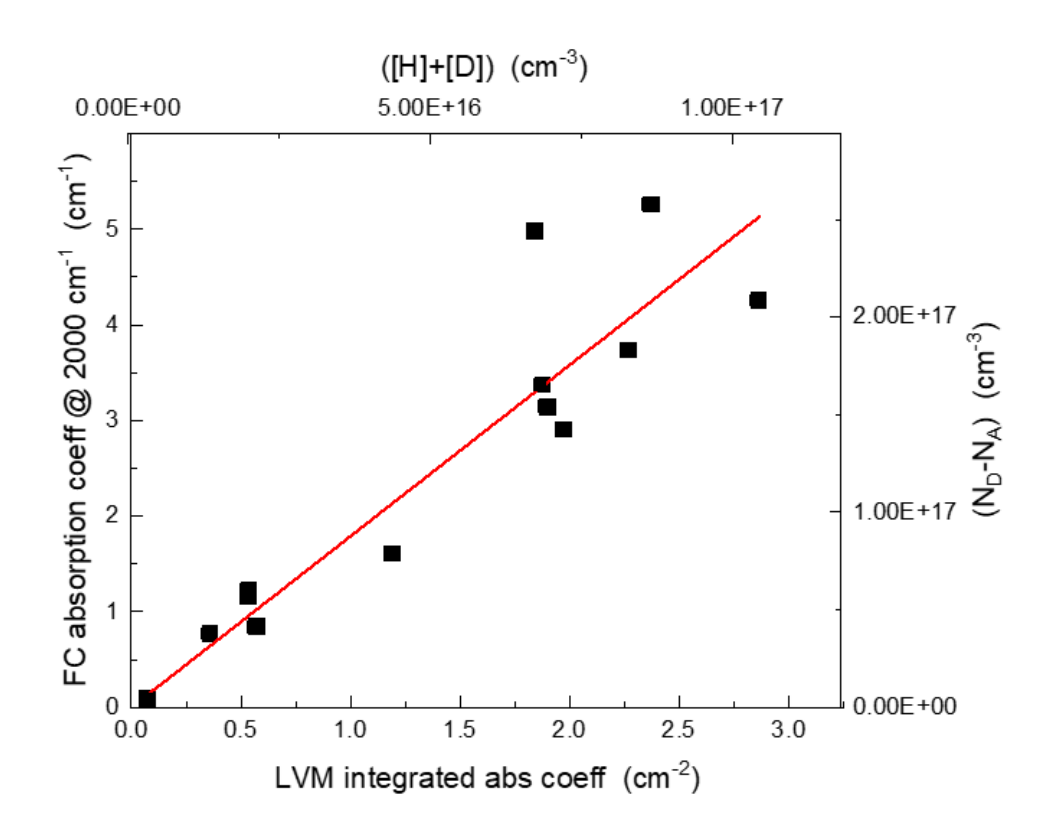
## **Applied Physics**

This is the author's peer reviewed, accepted manuscript. However, the online version of record will be different from this version once it has been copyedited and typeset.

PLEASE CITE THIS ARTICLE AS DOI: 10.1063/5.0160331

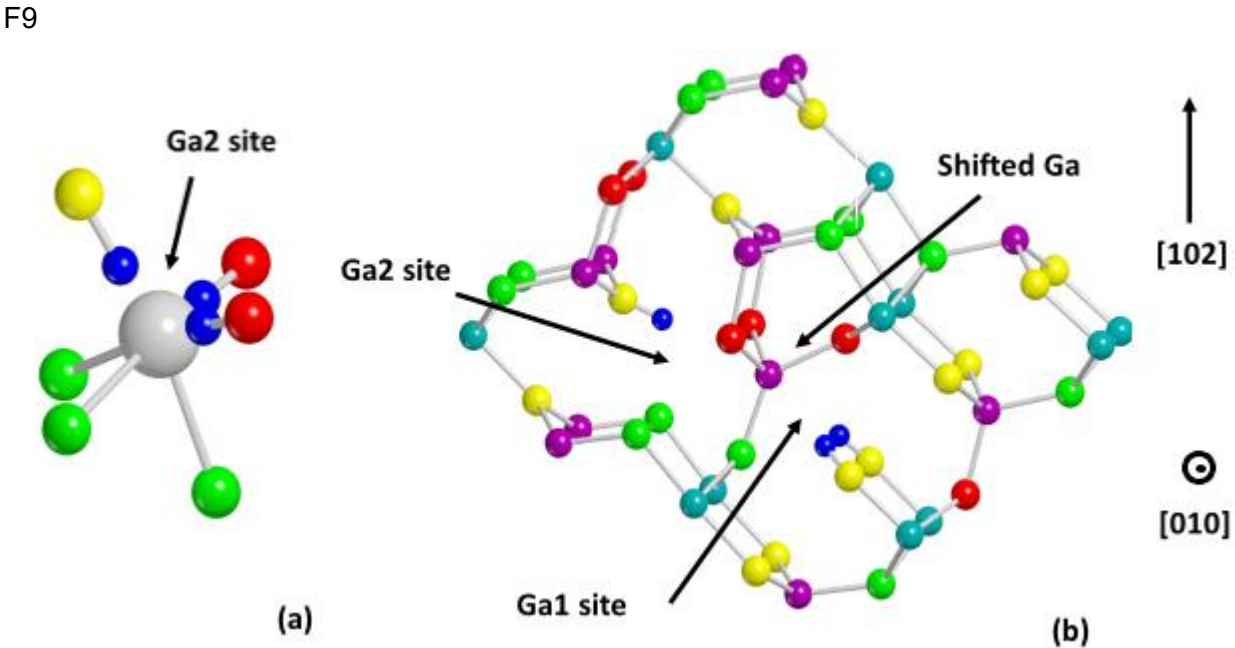


F7



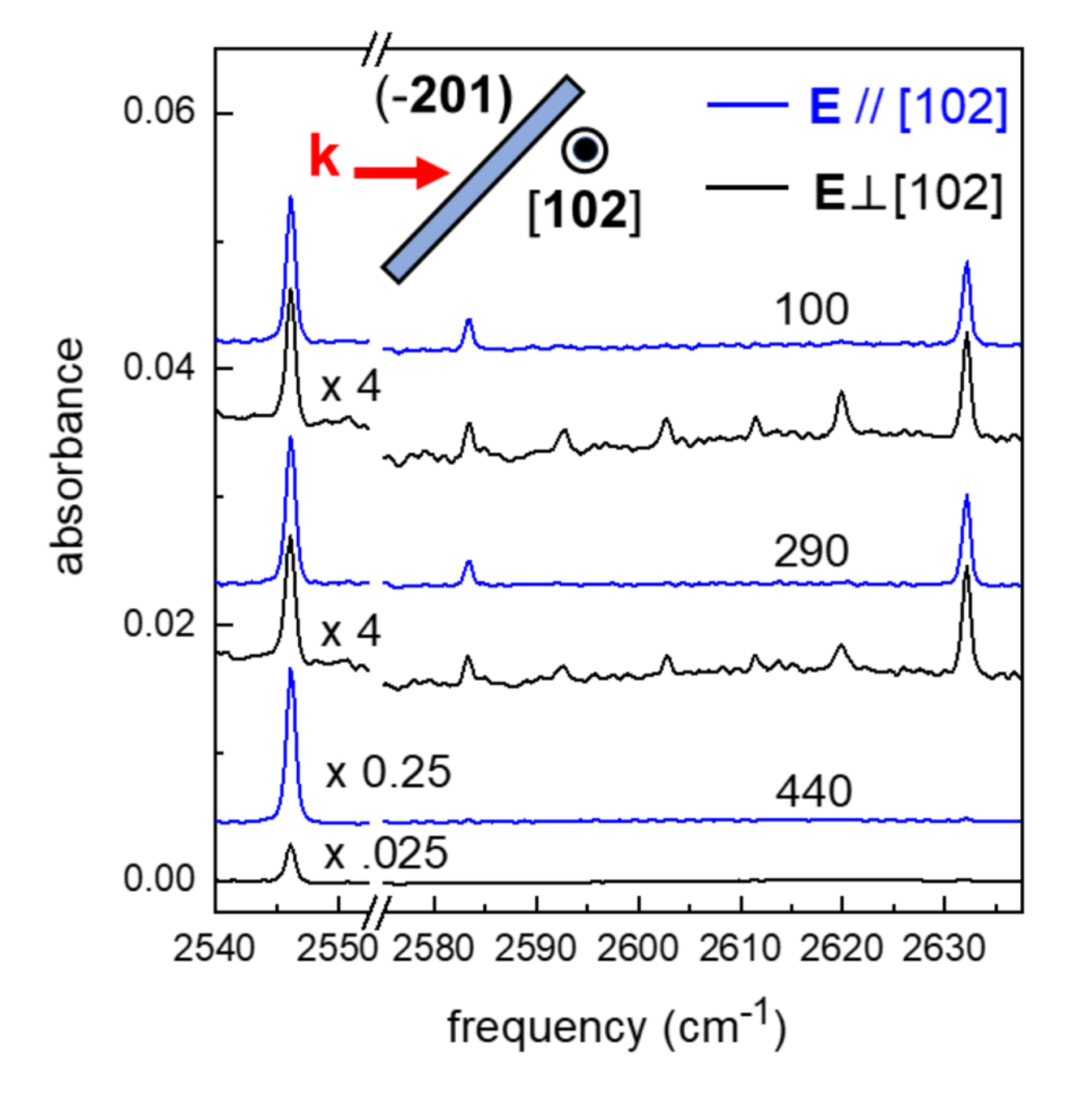
This is the author's peer reviewed, accepted manuscript. However, the online version of record will be different from this version once it has been copyedited and typeset. PLEASE CITE THIS ARTICLE AS DOI: 10.1063/5.0160331

(a) undoped β-Ga<sub>2</sub>O<sub>3</sub>  $V_{Ga1}^{ic} - nD$  + defect (2592, 2602, 2611, 2620 cm<sup>-1</sup>)  $V_{Ga1}^{ib} - D + \text{defect (2631 cm}^{-1})$  $V_{Ga1}^{ib} - 2D$  (2546 cm<sup>-1</sup>) (b) Cz-grown β-Ga<sub>2</sub>0<sub>3</sub>:Fe 2560 cm<sup>-1</sup>  $V_{Ga1}^{ib} - 2D$  (2546 cm<sup>-1</sup>)  $V_{Ga2} - nD$  or  $V_{Ga}^{ia} - nD$  (2467, 2475, 2493 cm<sup>-1</sup>)  $V_{Ga1}^{ib} - D + \text{defect (2631 cm}^{-1})$  $V_{Ga1}^{ic} - D$  + impurity (2577 cm<sup>-1</sup>) 200 400 600 800 0 T (°C)



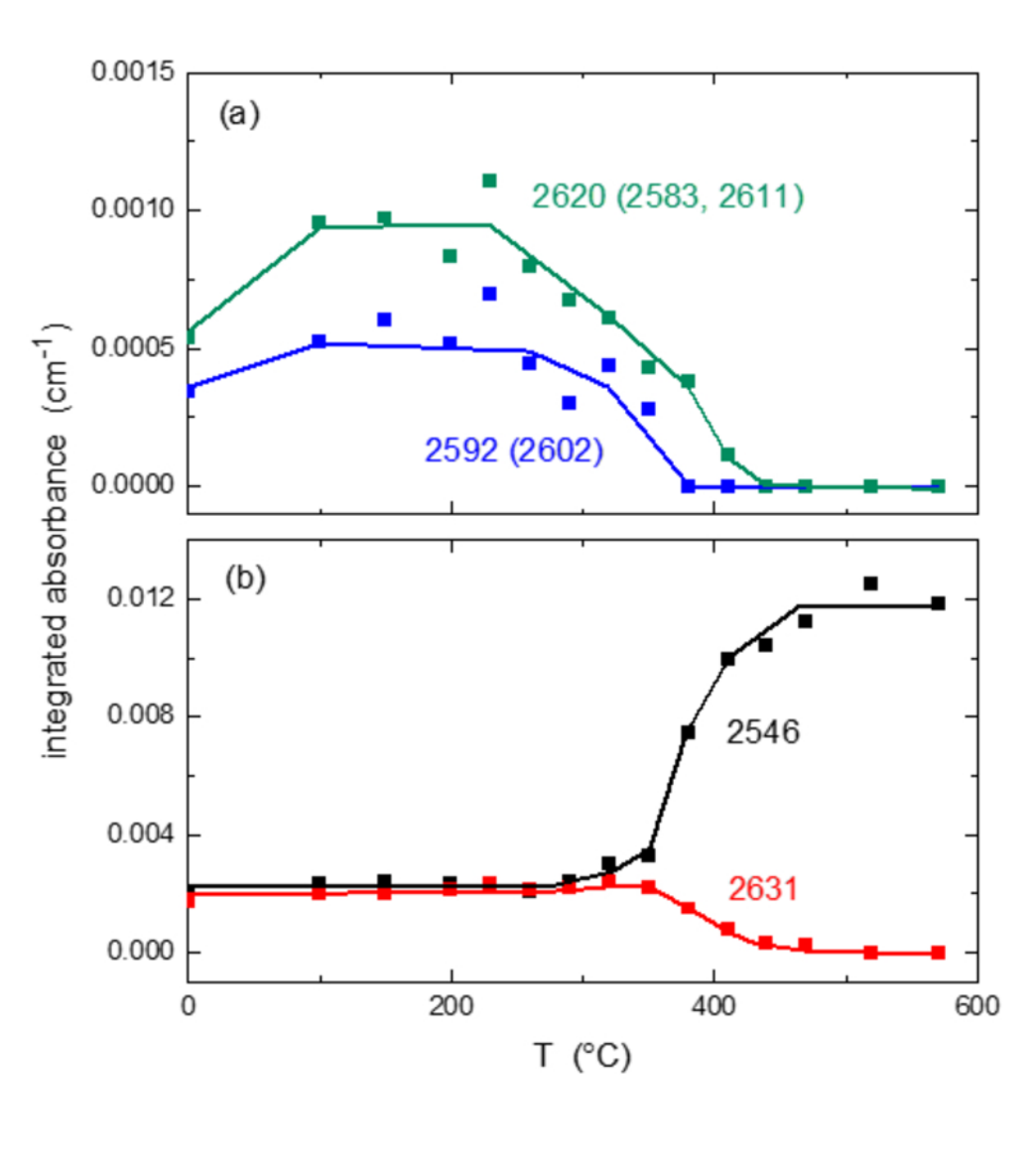
This is the author's peer reviewed, accepted manuscript. However, the online version of record will be different from this version once it has been copyedited and typeset.

PLEASE CITE THIS ARTICLE AS DOI: 10.1063/5.0160331



This is the author's peer reviewed, accepted manuscript. However, the online version of record will be different from this version once it has been copyedited and typeset.

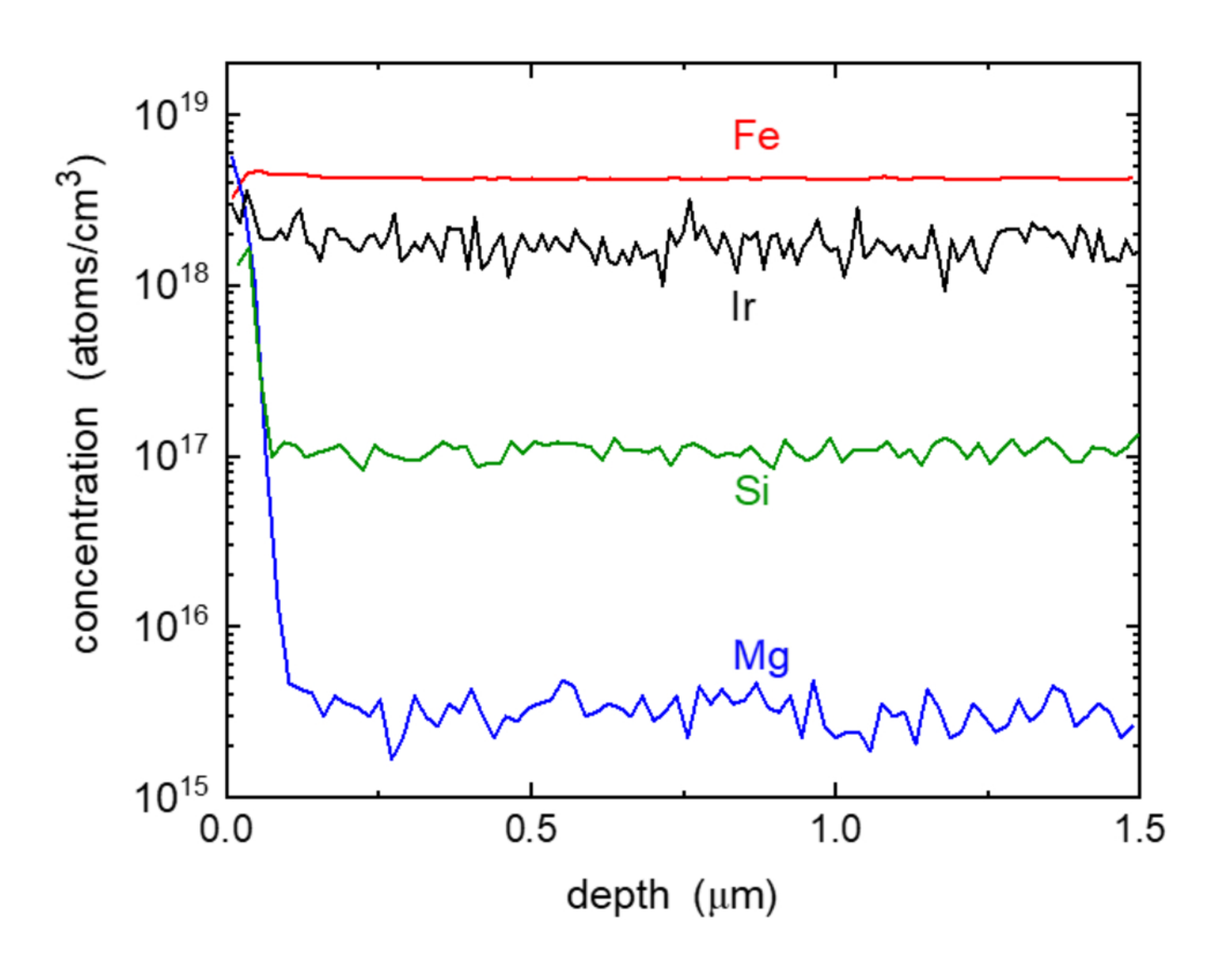
PLEASE CITE THIS ARTICLE AS DOI: 10.1063/5.0160331





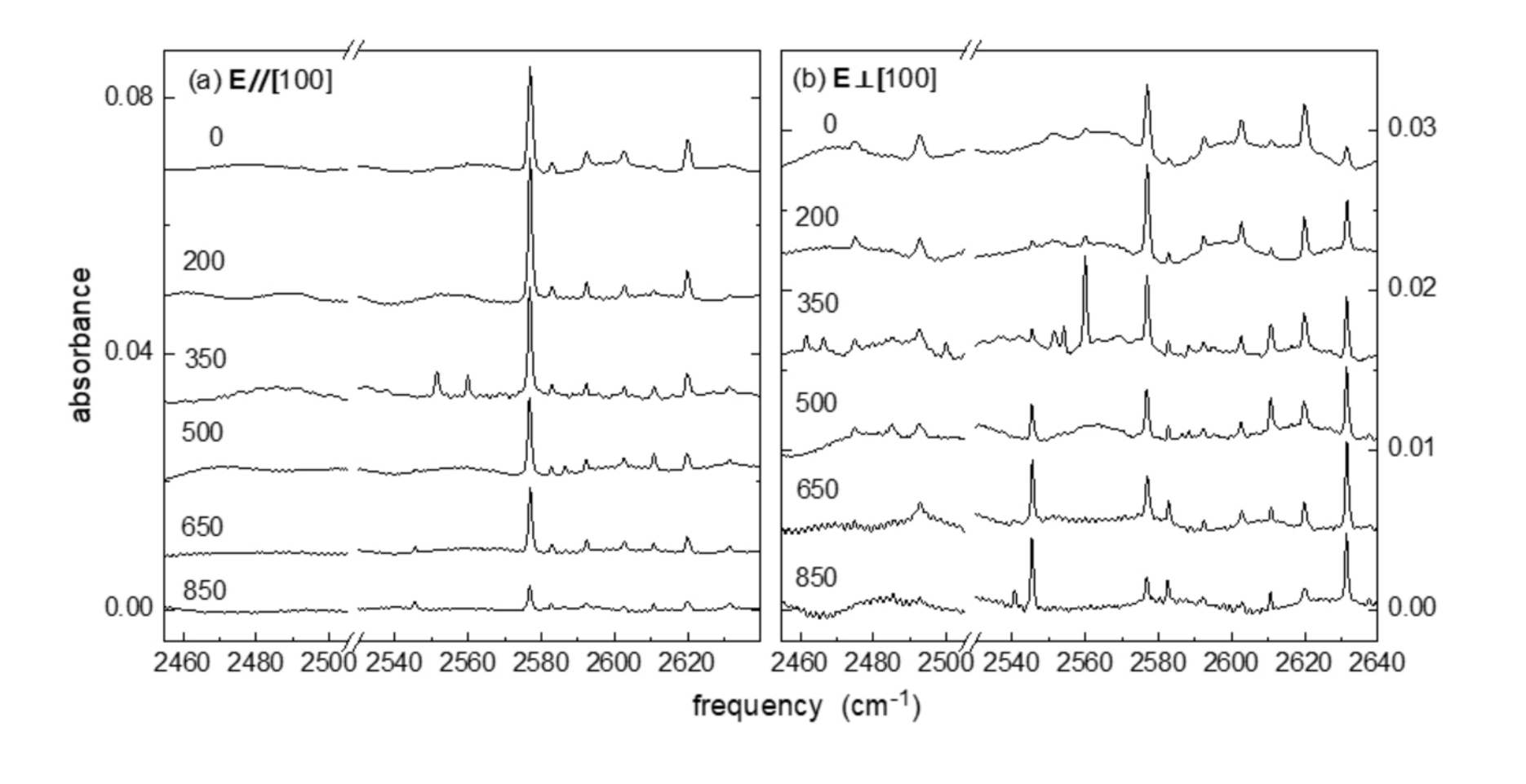
This is the author's peer reviewed, accepted manuscript. However, the online version of record will be different from this version once it has been copyedited and typeset.

PLEASE CITE THIS ARTICLE AS DOI: 10.1063/5.0160331



This is the author's peer reviewed, accepted manuscript. However, the online version of record will be different from this version once it has been copyedited and typeset.

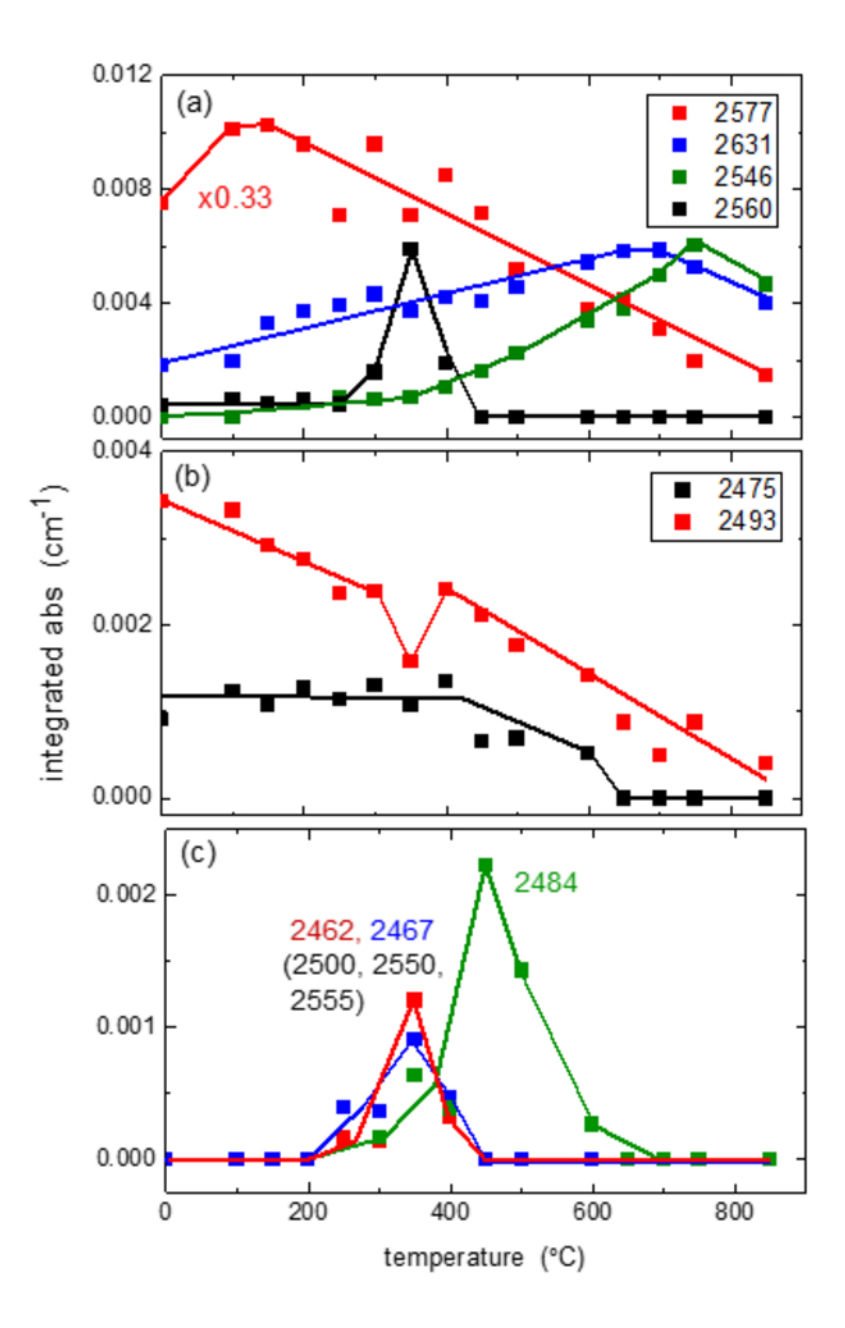
PLEASE CITE THIS ARTICLE AS DOI: 10.1063/5.0160331





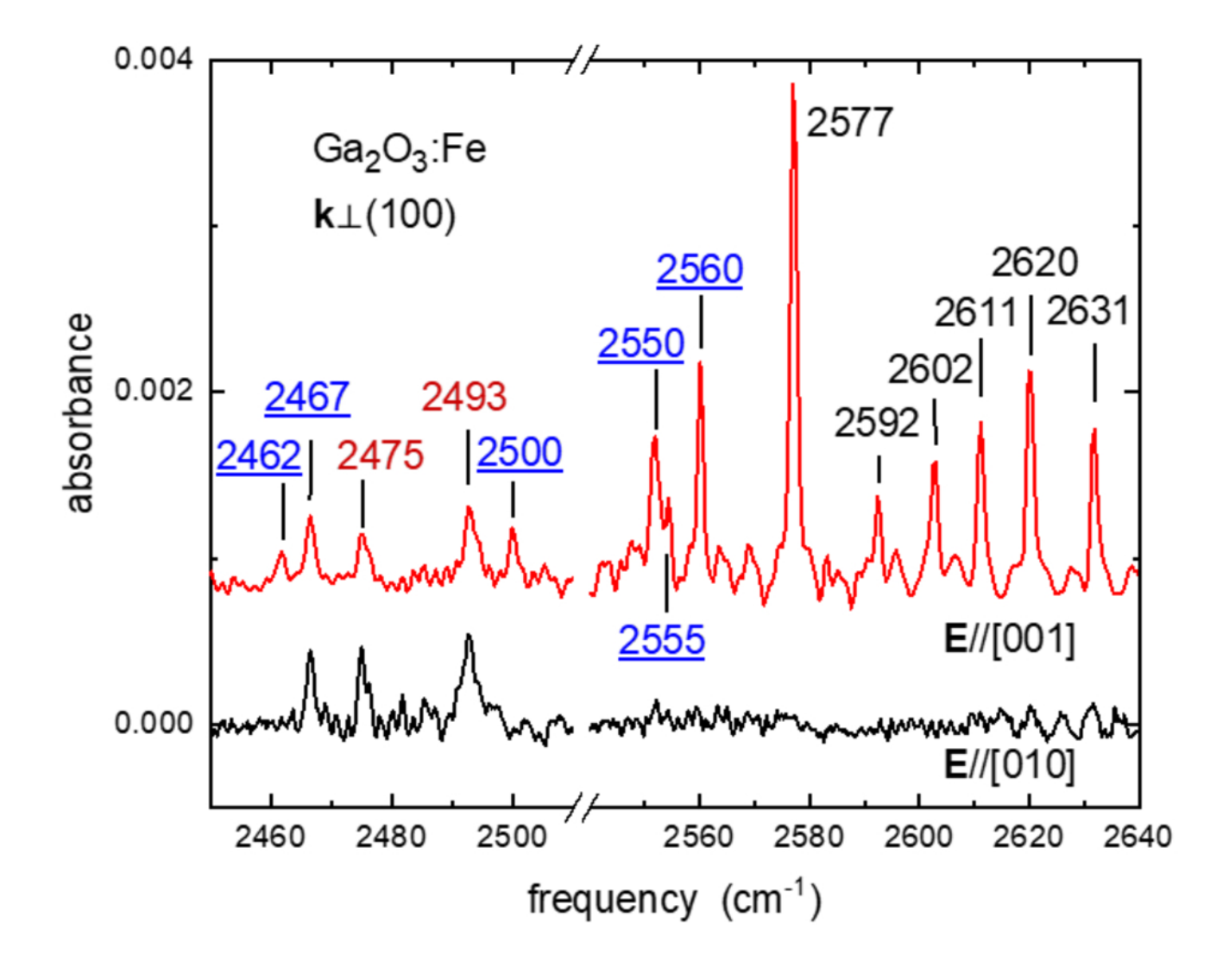
This is the author's peer reviewed, accepted manuscript. However, the online version of record will be different from this version once it has been copyedited and typeset.

PLEASE CITE THIS ARTICLE AS DOI: 10.1063/5.0160331



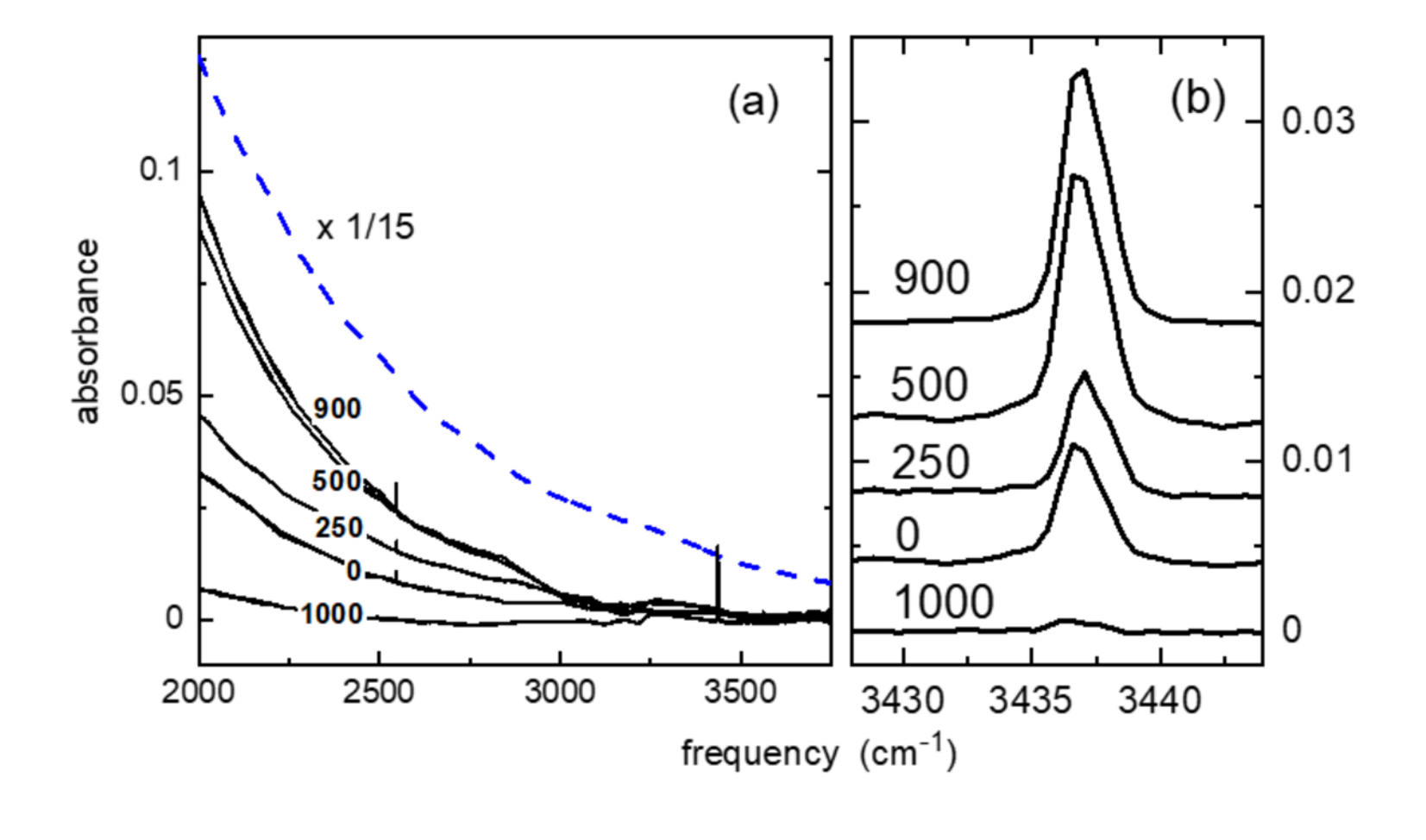
This is the author's peer reviewed, accepted manuscript. However, the online version of record will be different from this version once it has been copyedited and typeset.

PLEASE CITE THIS ARTICLE AS DOI: 10.1063/5.0160331



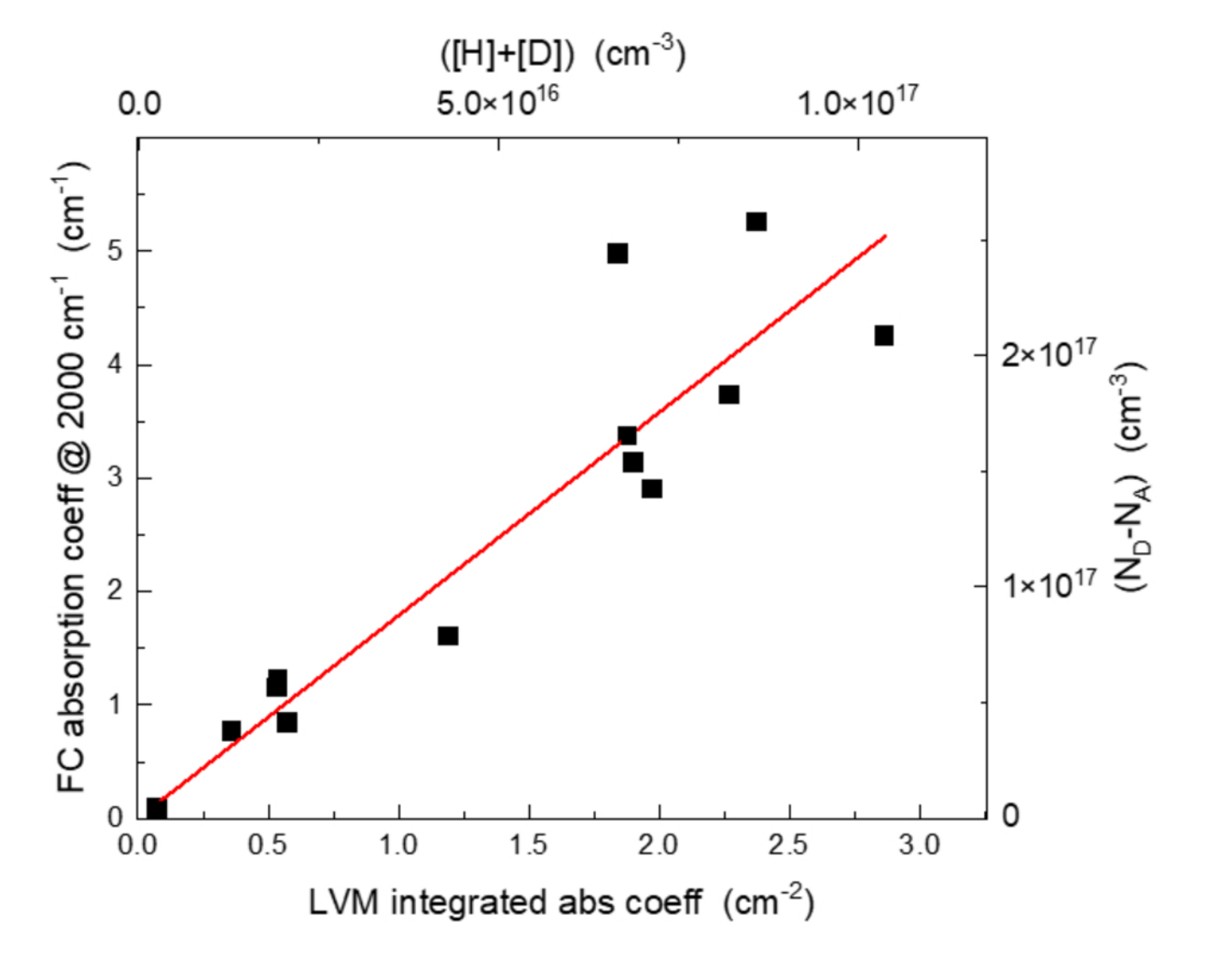
This is the author's peer reviewed, accepted manuscript. However, the online version of record will be different from this version once it has been copyedited and typeset.

PLEASE CITE THIS ARTICLE AS DOI: 10.1063/5.0160331



This is the author's peer reviewed, accepted manuscript. However, the online version of record will be different from this version once it has been copyedited and typeset.

PLEASE CITE THIS ARTICLE AS DOI: 10.1063/5.0160331



This is the author's peer reviewed, accepted manuscript. However, the online version of record will be different from this version once it has been copyedited and typeset.

PLEASE CITE THIS ARTICLE AS DOI: 10.1063/5.0160331

(a) undoped β-Ga<sub>2</sub>O<sub>3</sub>  $V_{Ga1}^{ic} - nD$  + defect (2592, 2602, 2611, 2620 cm<sup>-1</sup>)  $V_{Ga1}^{ib} - D + \text{defect (2631 cm}^{-1})$  $V_{Ga1}^{ib} - 2D$  (2546 cm<sup>-1</sup>) (b) Cz-grown β-Ga<sub>2</sub>0<sub>3</sub>:Fe 2560 cm<sup>-1</sup>  $V_{Ga1}^{ib}-2D$  $V_{Ga2}-nD$  or  $V_{Ga}^{ia}-nD$ (2546 cm<sup>-1</sup>) (2467, 2475, 2493 cm<sup>-1</sup>)  $V_{Ga1}^{ib} - D + \text{defect (2631 cm}^{-1})$ 

600

800

 $V_{Ga1}^{ic} - D$  + impurity (2577 cm<sup>-1</sup>)

400

T (°C)

200

This is the author's peer reviewed, accepted manuscript. However, the online version of record will be different from this version once it has been copyedited and typeset.

PLEASE CITE THIS ARTICLE AS DOI: 10.1063/5.0160331

Ga2 site **Shifted Ga** [102] Ga2 site 0 [010] Ga1 site (a) (b)

This is the author's peer reviewed, accepted manuscript. However, the online version of record will be different from this version once it has been copyedited and typeset.

PLEASE CITE THIS ARTICLE AS DOI: 10.1063/5.0160331

Ga2 site **Shifted Ga** [102] Ga2 site 0 [010] Ga1 site (a) (b)